Supporting Information

pH-induced Linkage Isomerism of Pd(II) complexes: A Pathway to Air- and Water-Stable Suzuki-Miyaura Reaction Catalysts

Anna Walczak[†‡] and Artur R. Stefankiewicz[†‡*]

† Faculty of Chemistry, Adam Mickiewicz University, ul. Umultowska 89b, 61-614 Poznań, Poland. ; Tel: +48618291678; E-mail: ars@amu.edu.pl

‡ Centre for Advanced Technologies, Adam Mickiewicz University, ul. Umultowska 89c, 61-614 Poznań, Poland.

Table of Contents

1. NMR Spectroscopic and TOF-MS Analysis

Ligand L1

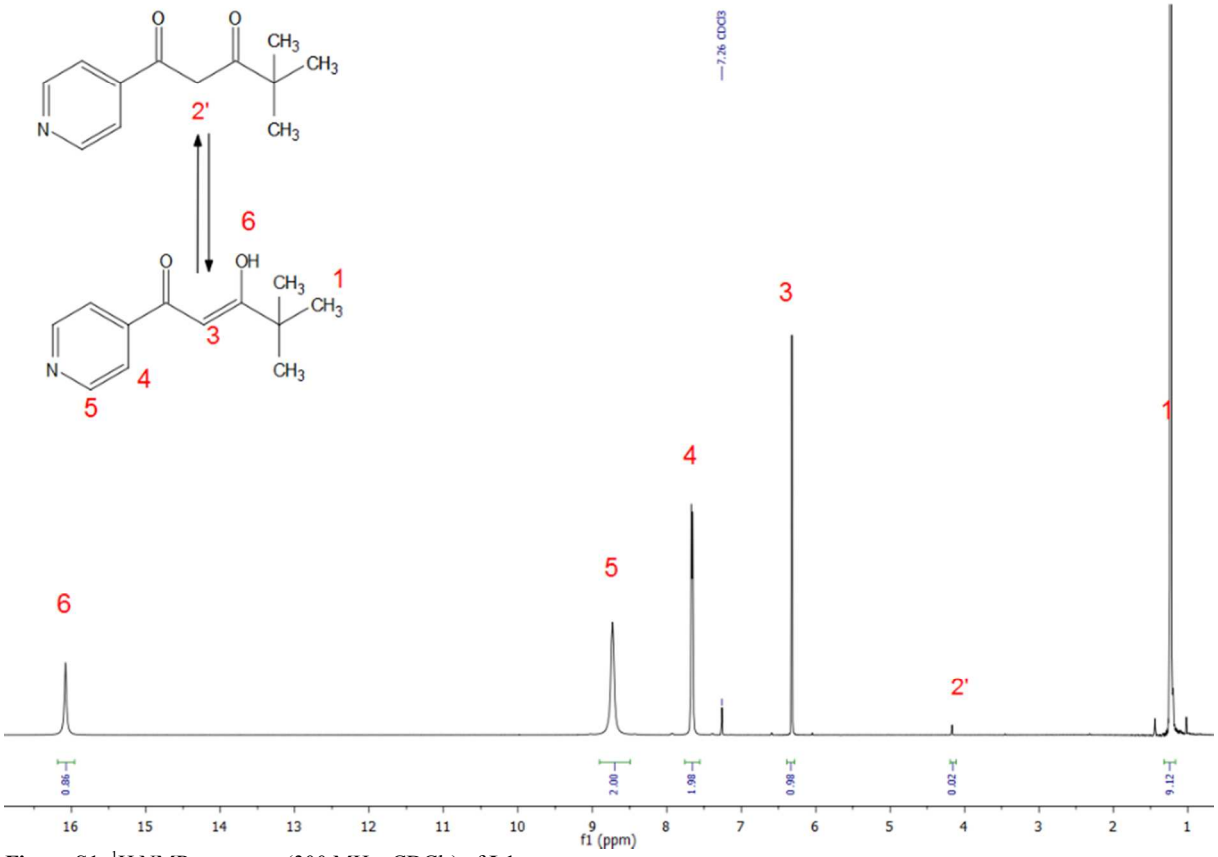

Figure S1. ^{1}H NMR spectrum (300 MHz, $CDCl_3$) of **L1**.

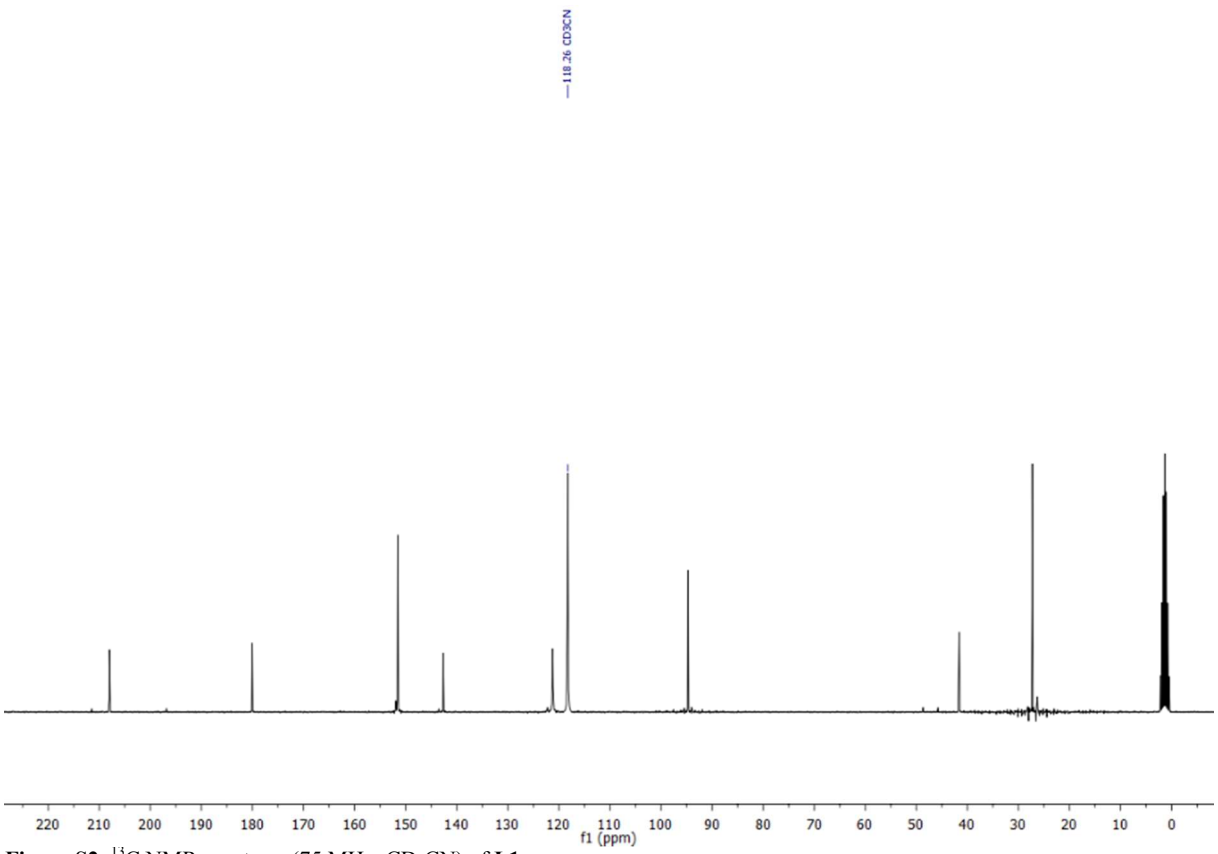

Figure S2. ^{13}C NMR spectrum (75 MHz, CD_3CN) of **L1**.

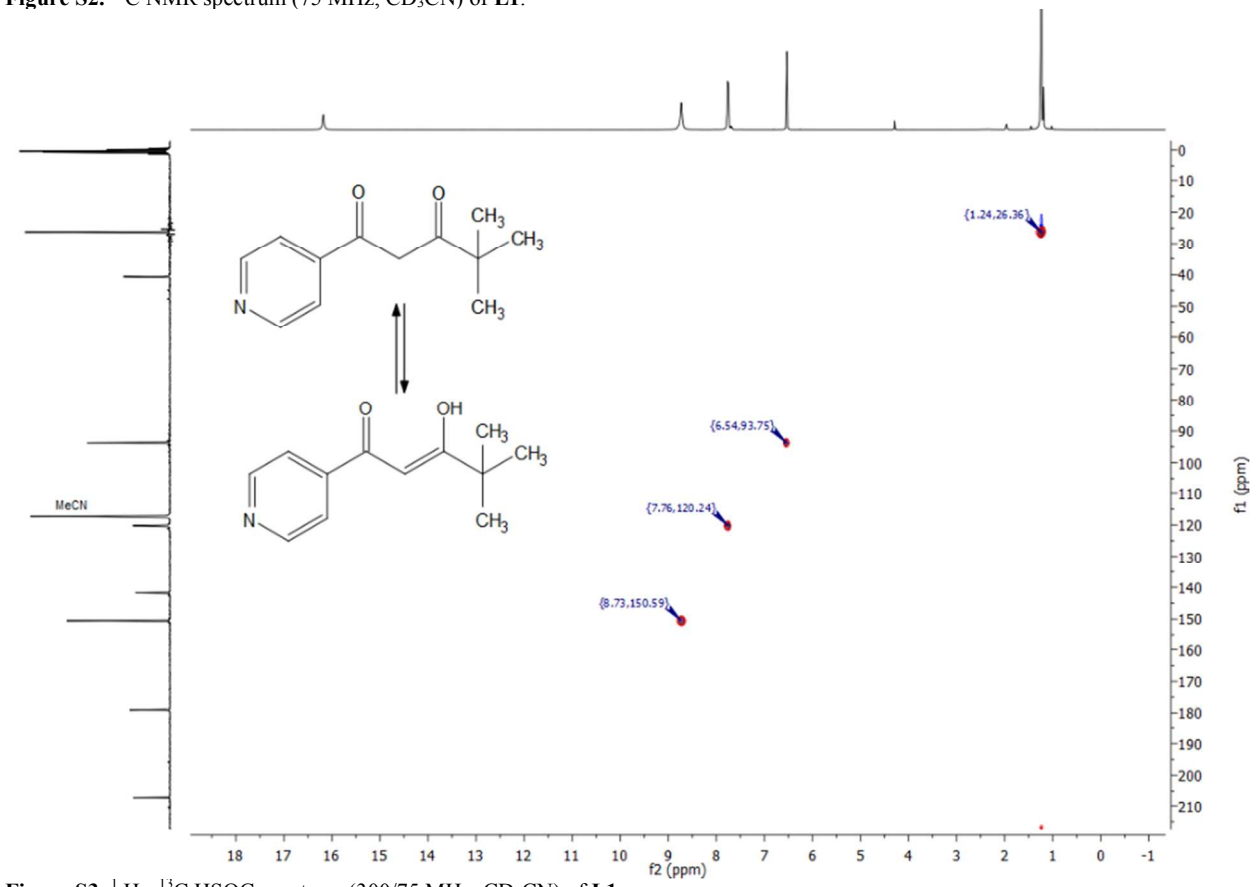

Figure S3. ^{1}H - ^{13}C HSQC spectrum (300/75 MHz, CD_3CN) of **L1**.

Ligand L2

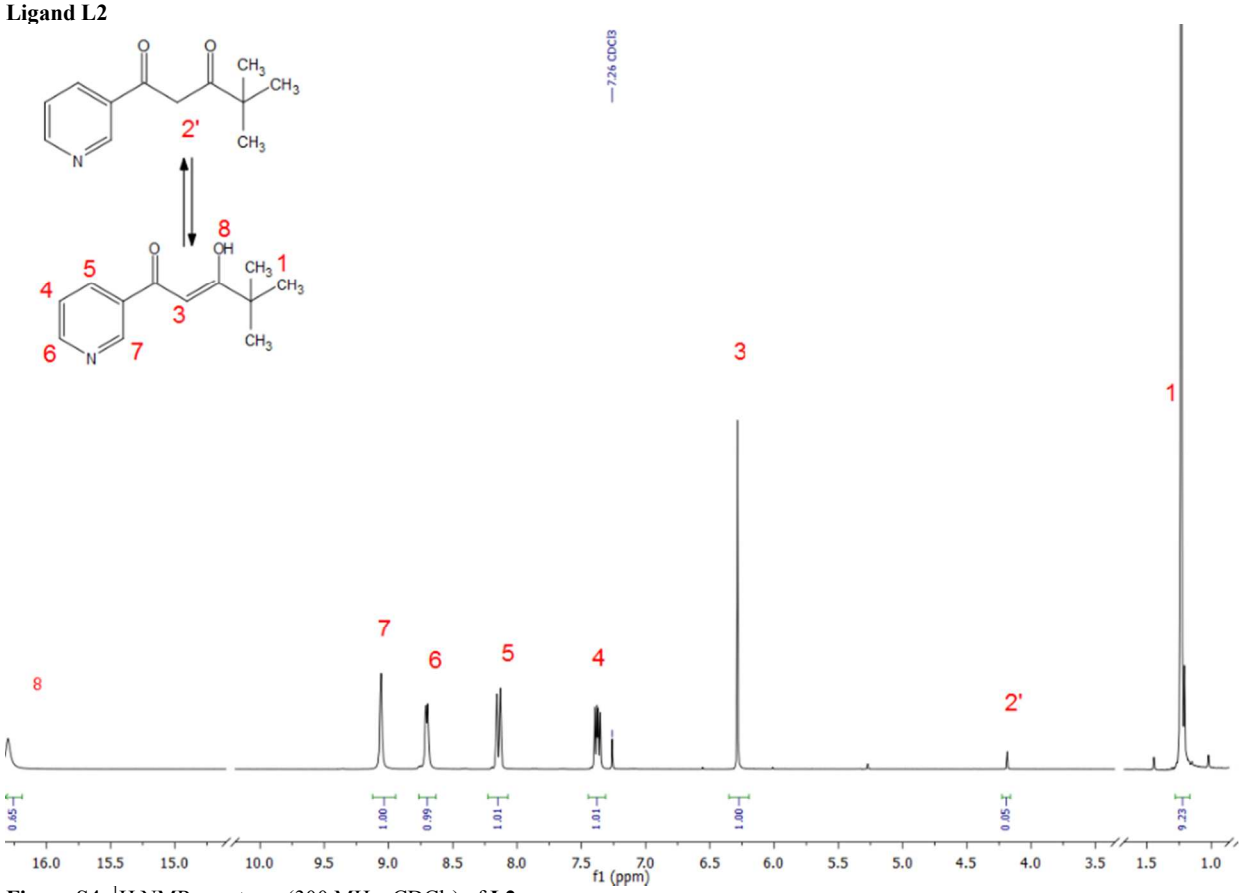

Figure S4. ^{1}H NMR spectrum (300 MHz, $CDCl_3$) of **L2**.

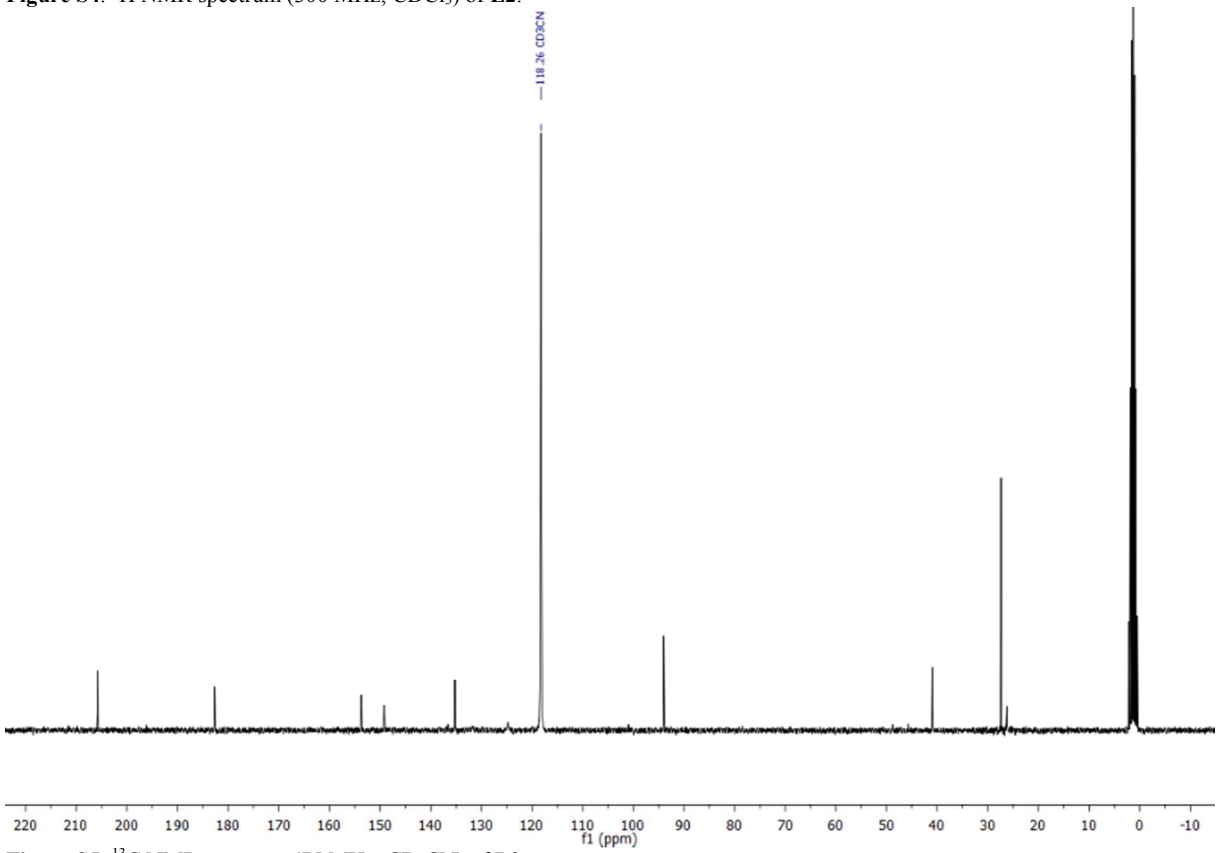

Figure S5. ^{13}C NMR spectrum (75 MHz, CD_3CN) of **L2**.

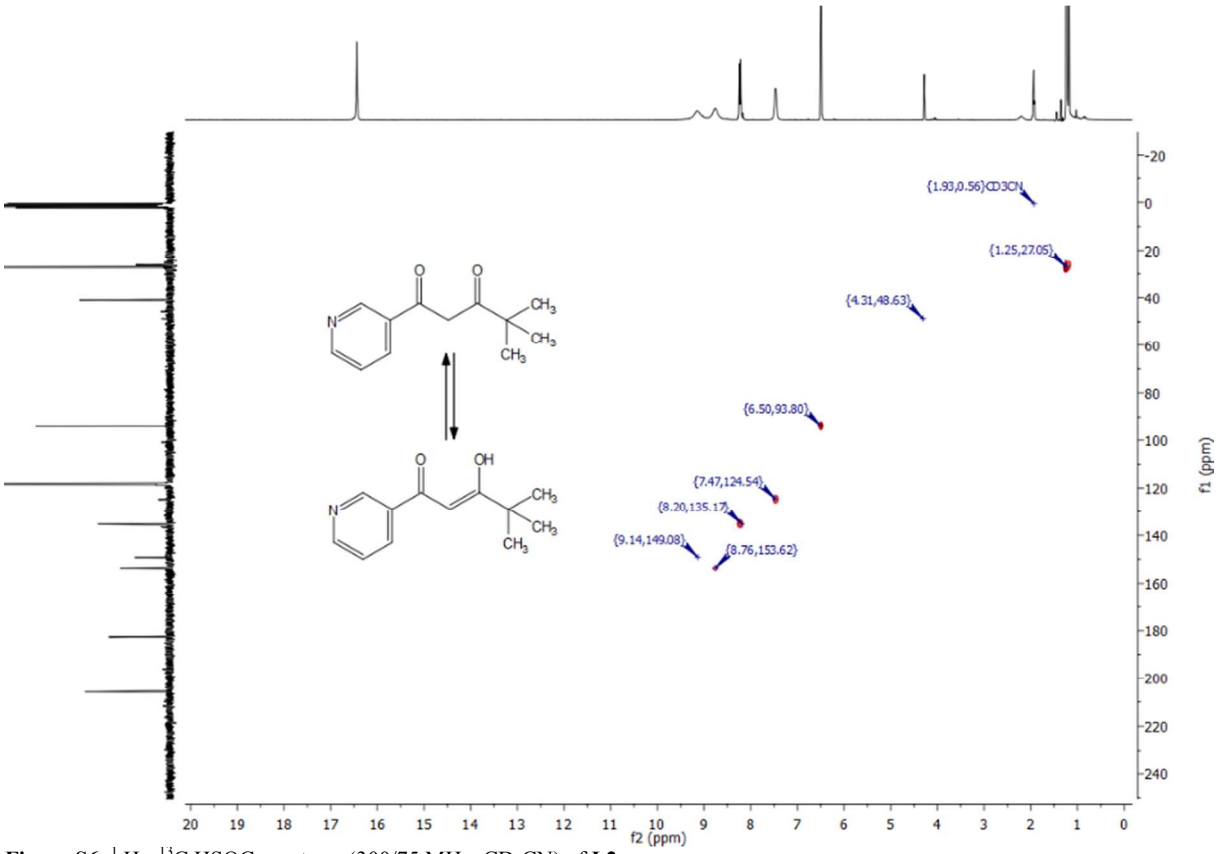

Figure S6. ^{1}H - ^{13}C HSQC spectrum (300/75 MHz, CD_3CN) of **L2**.

Complex 1

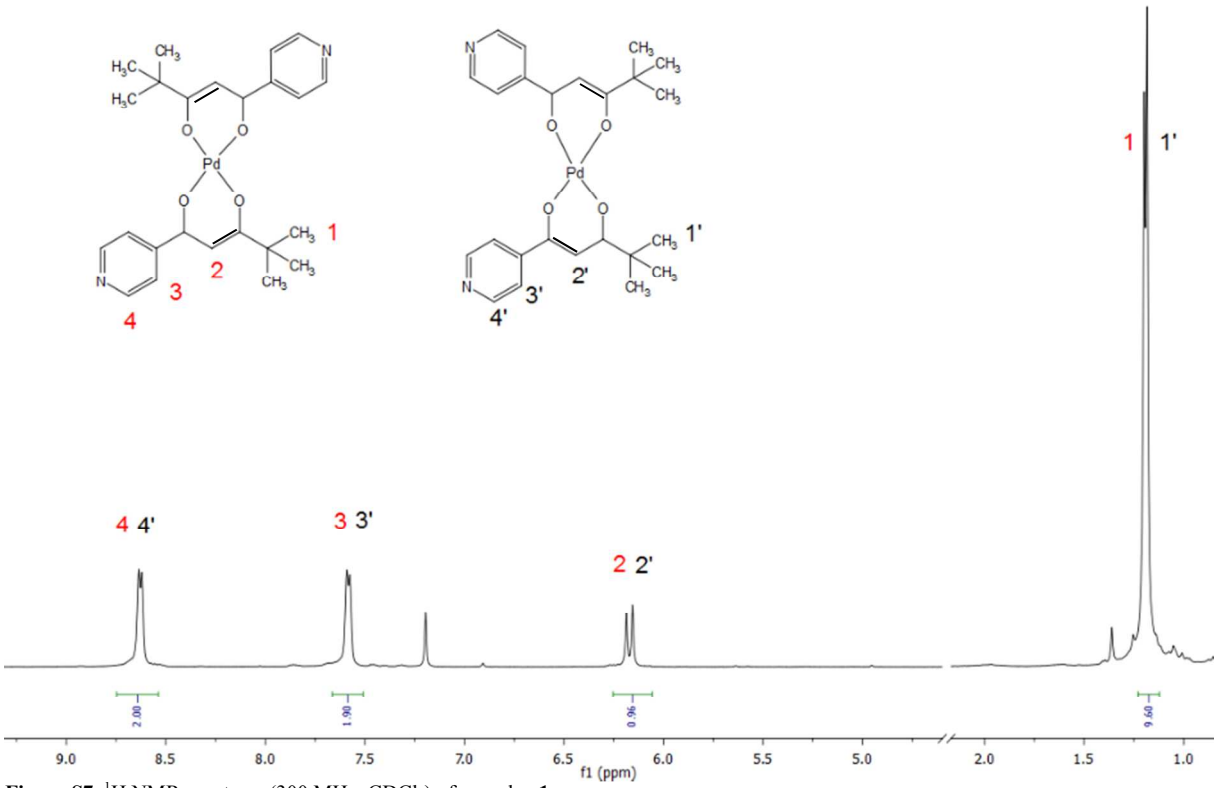

Figure S7. ^{1}H NMR spectrum (300 MHz, $CDCl_3$) of complex **1**.

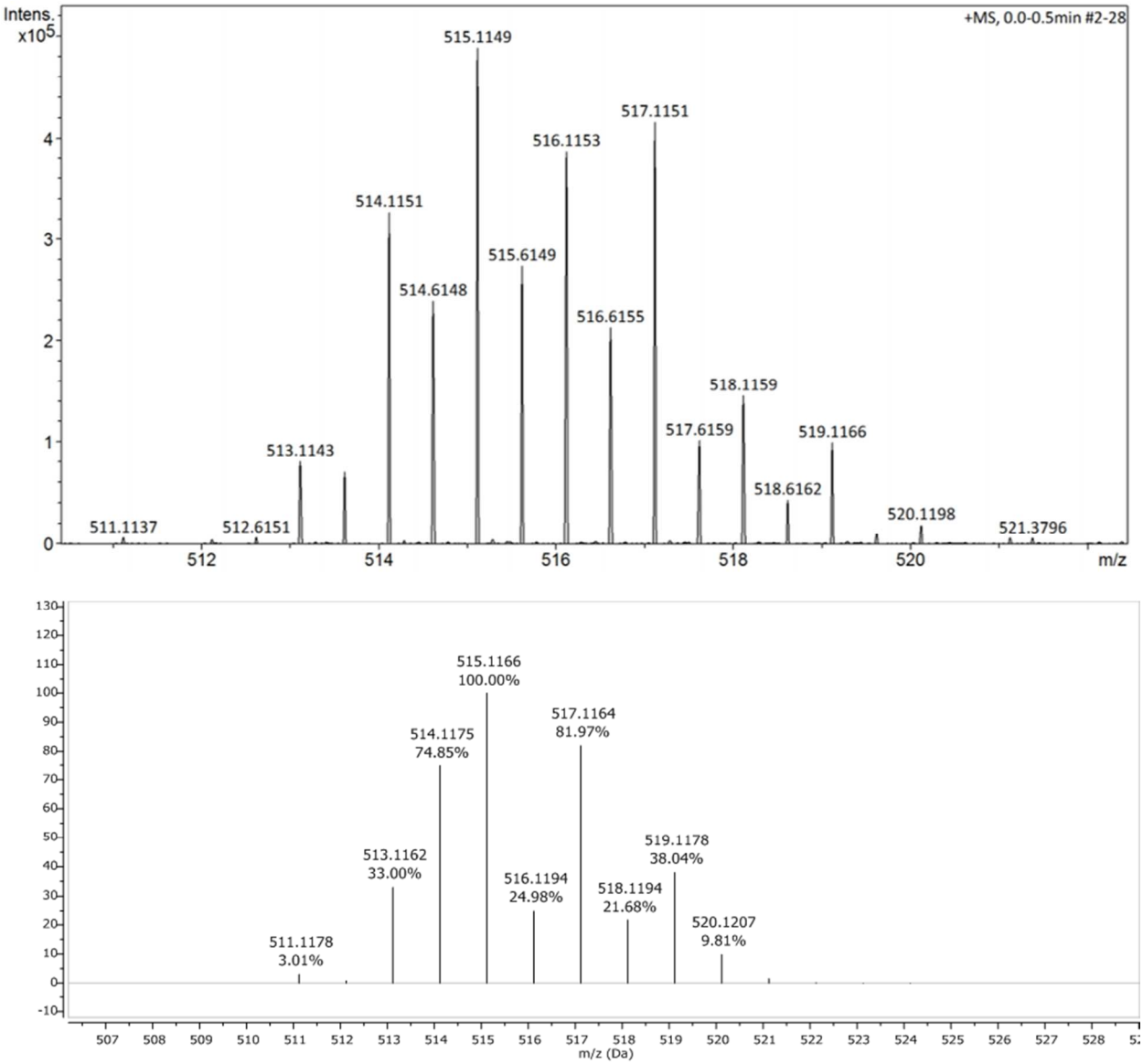

Figure S8. TOF-MS analysis of **1**, showing the observed data (bottom) and the theoretical isotope model (top).

Complex 2

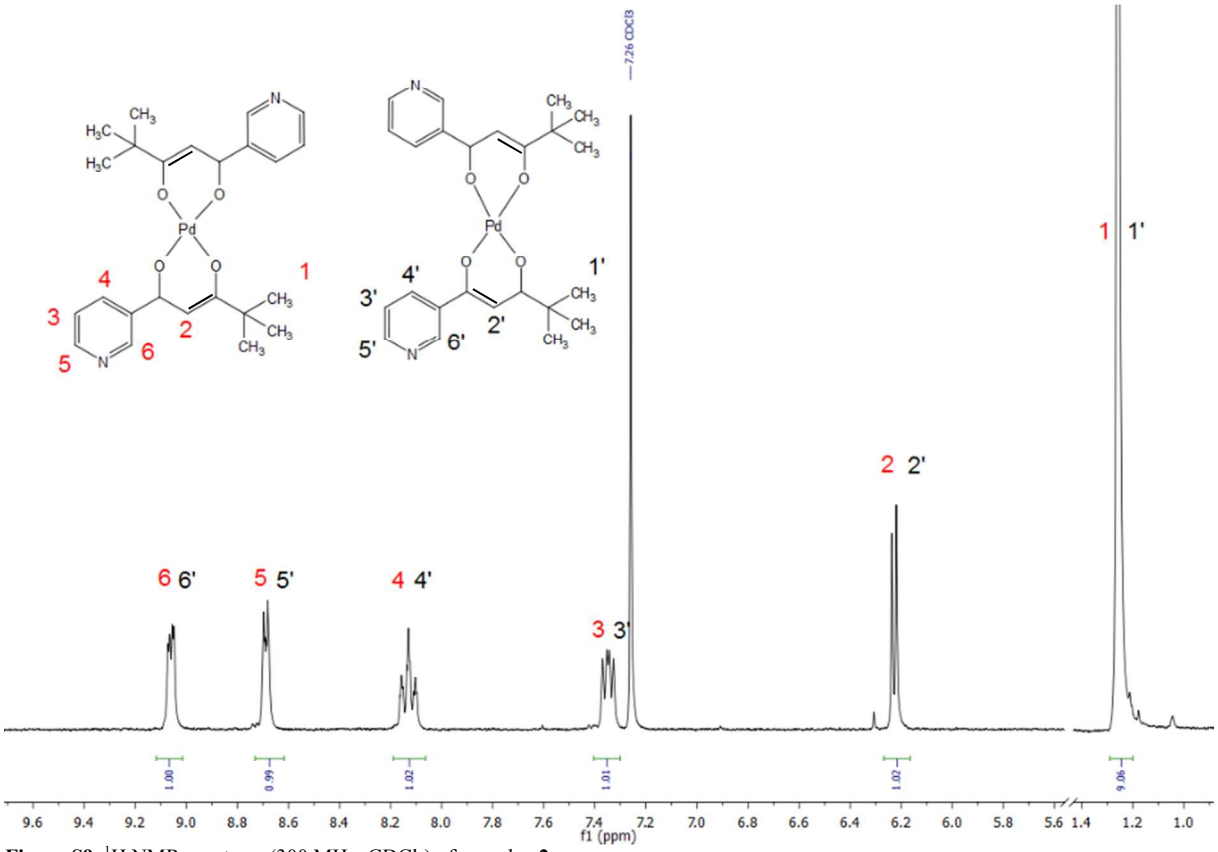

Figure S9. ^{1}H NMR spectrum (300 MHz, $CDCl_3$) of complex **2**.

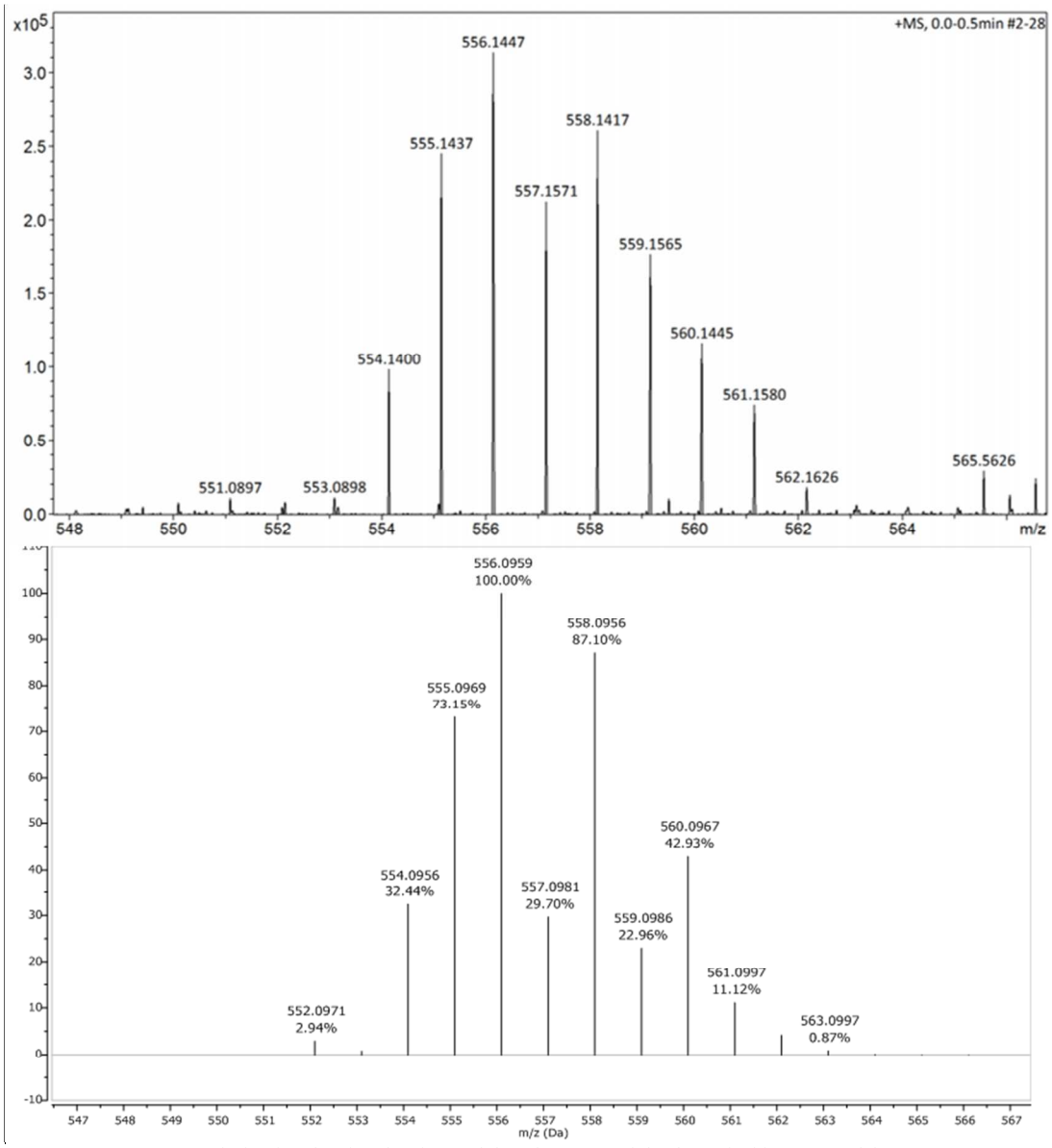

Figure S10. TOF-MS analysis of **2**, showing the observed data (bottom) and the theoretical isotope model (top).

Complex 3

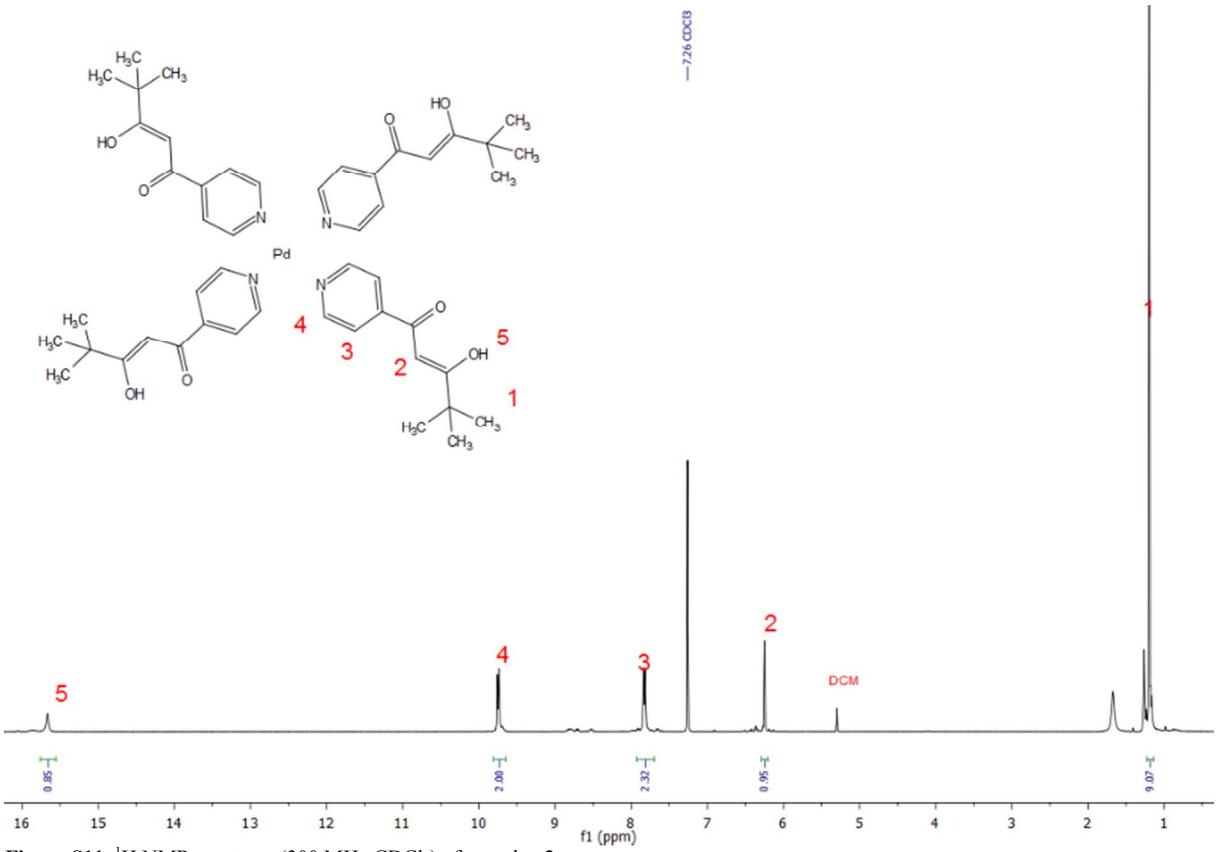

Figure S11. ^{1}H NMR spectrum (300 MHz,$CDCl_3$) of complex **3**.

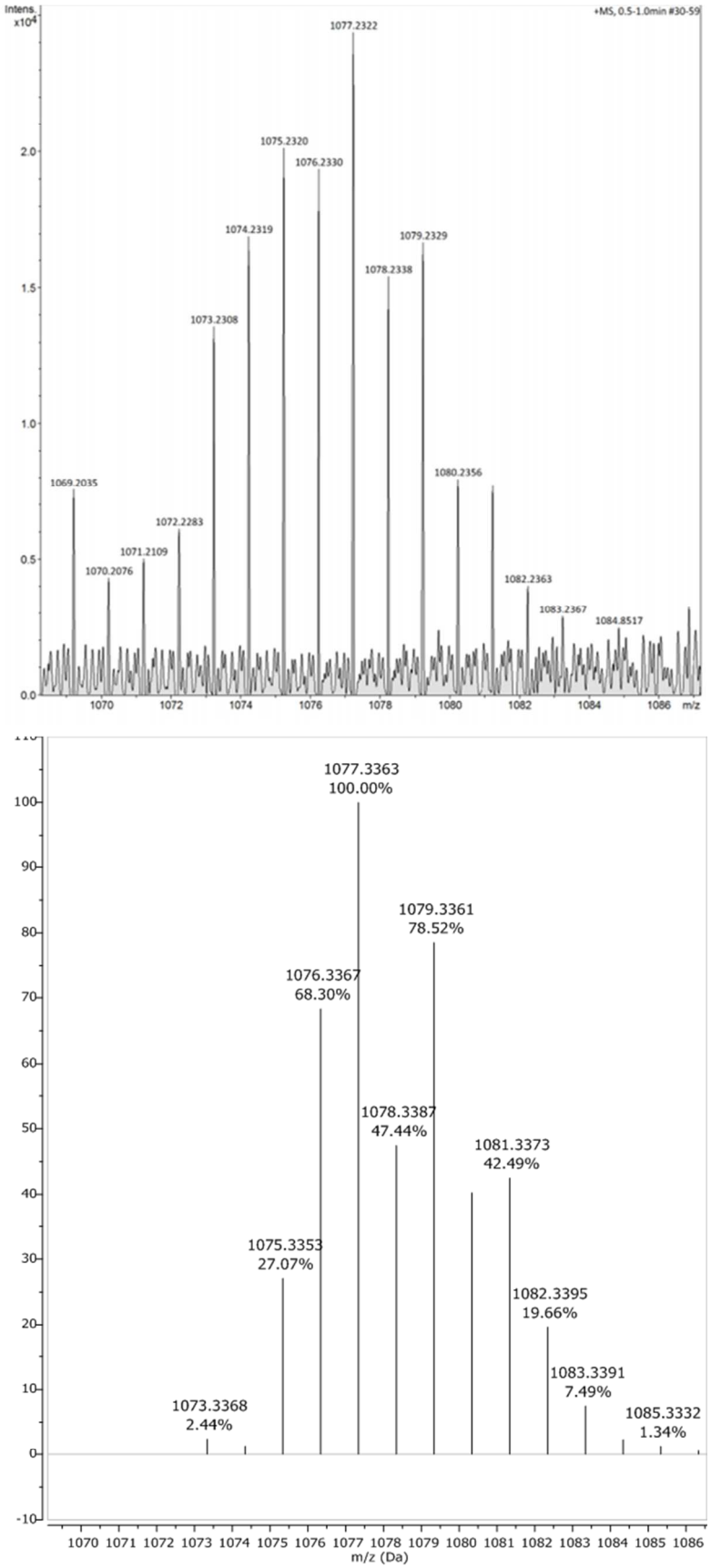

Figure S12. TOF-MS analysis of **3**, showing the observed data (bottom) and the theoretical isotope model (top).

Complex 4

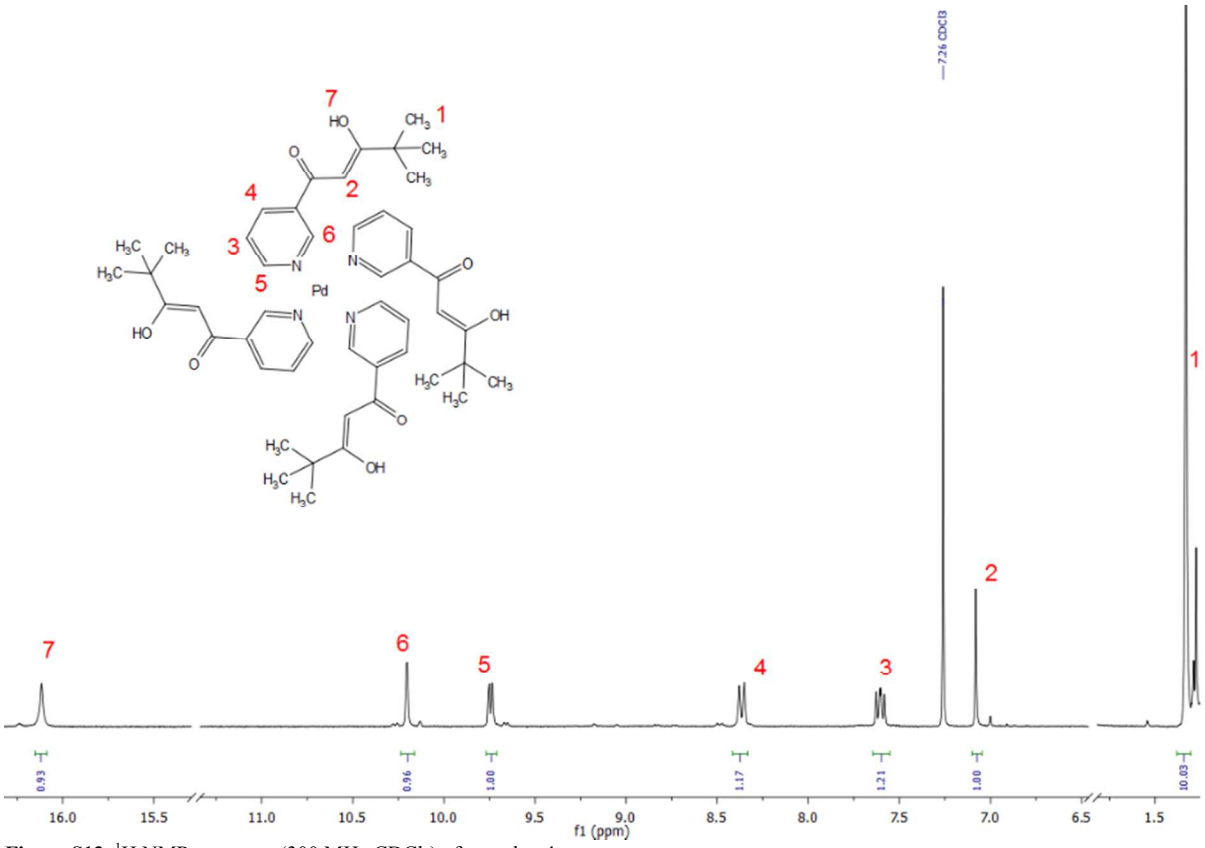

Figure S13. ^{1}H NMR spectrum (300 MHz,$CDCl_3$) of complex **4**.

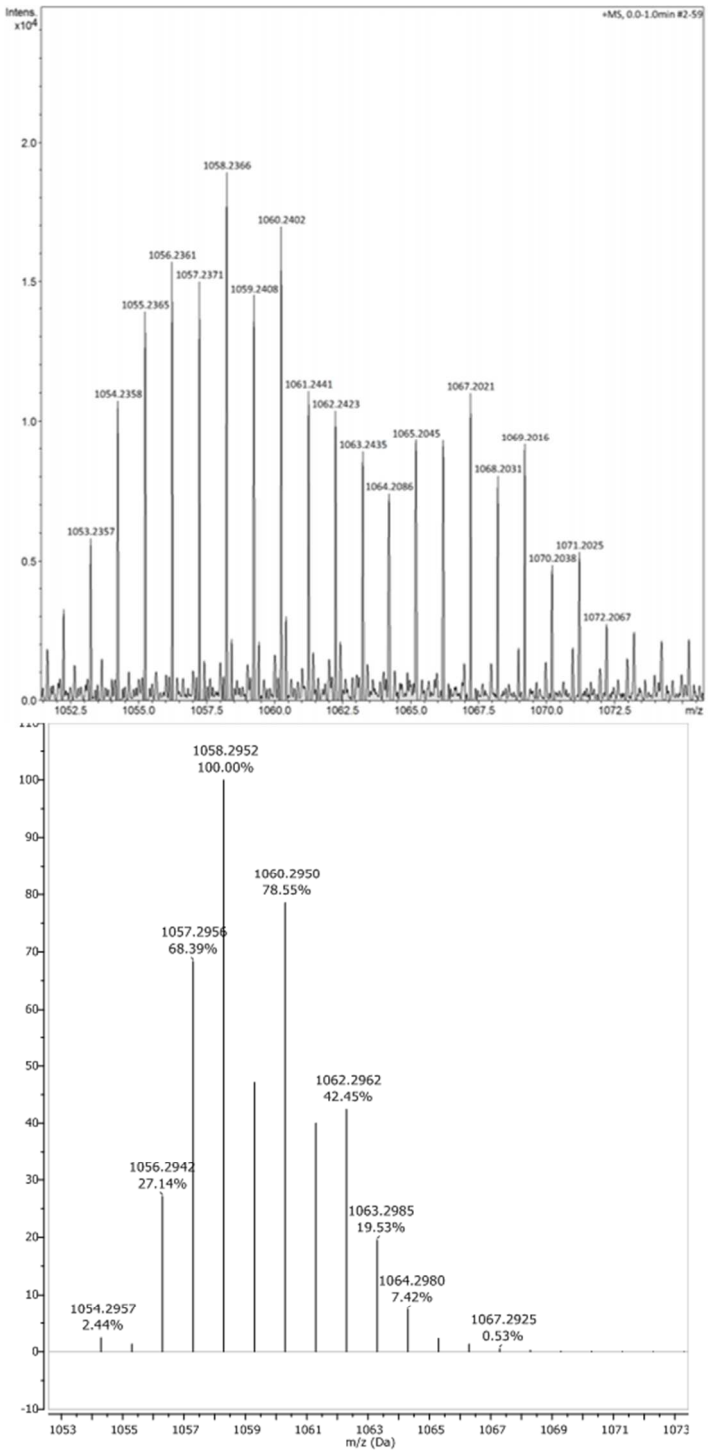

Figure S14. TOF-MS analysis of **4**, showing the observed data (bottom) and the theoretical isotope model (top).

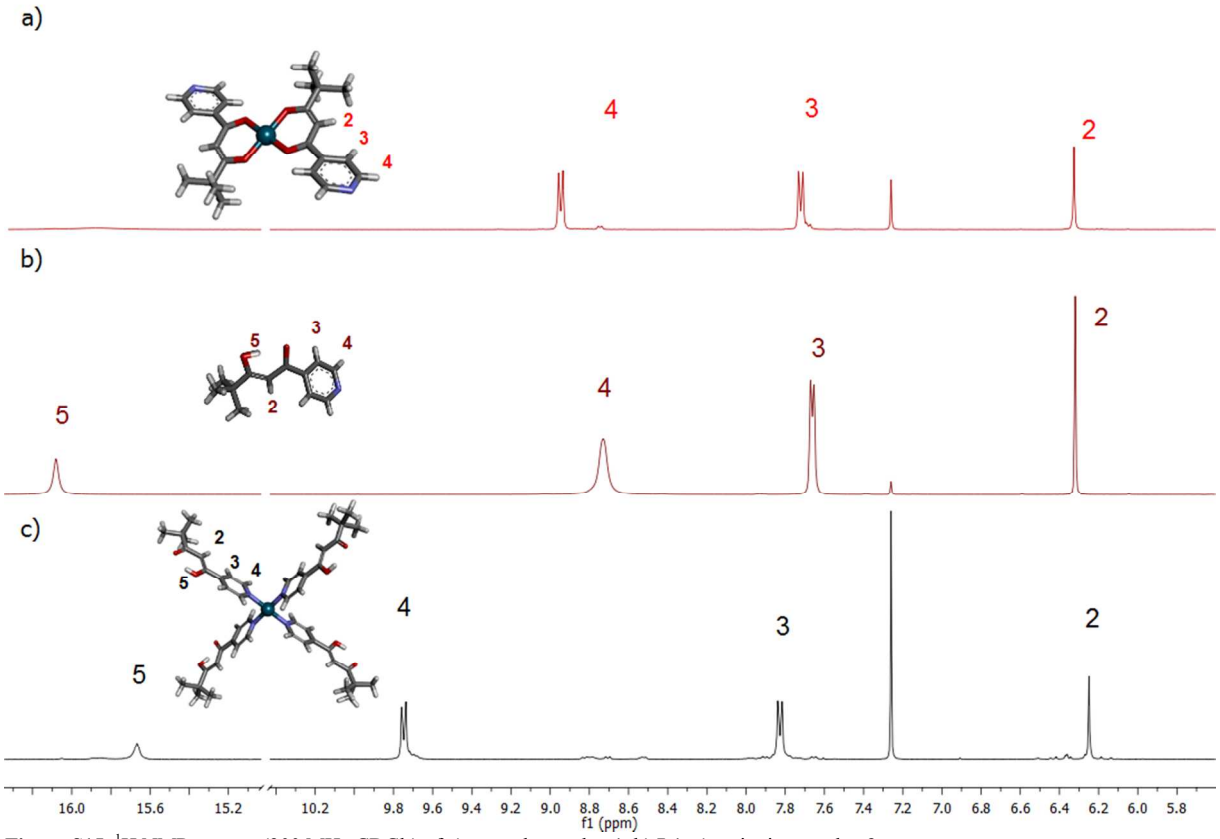

Figure S15. ^{1}H NMR spectra (300 MHz,$CDCl_3$) of a) neutral complex **1**, b) **L1**, c) cationic complex **3**.

2. X-ray Crystal Structure Analysis

Ligand L1

Table S1. Crystal data and structure refinement for ligand L1.

Identification code	Ligand L1
Empirical formula	$C_{12}H_{15}NO_2$
Formula weight	205.25
Temperature/K	294.5(8)
Crystal system	orthorhombic
Space group	Pbca
a/Å	11.4449(3)
b/Å	11.3204(2)
c/Å	35.6663(9)
α/°	90
β/°	90
γ/°	90
Volume/Å^3	4620.96(19)
Z	16
ρ_{calc}g/cm^3	1.180
μ/mm^{-1}	0.080
F(000)	1760.0
Crystal size/mm^3	0.3 × 0.2 × 0.1
Radiation	MoKα (λ = 0.71073)
2Θ range for data collection/°	8.302 to 50.05
Index ranges	-13 ≤ h ≤ 13, -13 ≤ k ≤ 13, -41 ≤ l ≤ 41
Reflections collected	49793

Independent reflections	4000 [R_{int} = 0.0251, R_{sigma} = 0.0114]
Data/restraints/parameters	4000/0/282
Goodness-of-fit on F^2	1.052
Final R indexes [I>=2σ (I)]	R_1 = 0.0506, wR_2 = 0.1365
Final R indexes [all data]	R_1 = 0.0670, wR_2 = 0.1485
Largest diff. peak/hole / e Å^{-3}	0.30/-0.18

Crystal structure determination of [Ligand L1]

Crystal Data for $C_{12}H_{15}NO_2$ (*M* =205.25 g/mol): orthorhombic, space group Pbca (no. 61), *a* = 11.4449(3) Å, *b* = 11.3204(2) Å, *c* = 35.6663(9) Å, *V* = 4620.96(19) Å^3, *Z* = 16, *T* = 294.5(8) K, μ(MoKα) = 0.080 mm^{-1}, *Dcalc* = 1.180 g/cm^3, 49793 reflections measured (8.302° ≤ 2Θ ≤ 50.05°), 4000 unique (R_{int} = 0.0251, R_{sigma} = 0.0114) which were used in all calculations. The final R_1 was 0.0506 (I > 2σ(I)) and wR_2 was 0.1485 (all data).

CheckCif alert is listed according to Alert Level B for compound L1

PLAT355_ALERT_3_B Long O-H (X0.82,N0.98A) O1' - H1' .. 1.09 Ang.
Response: Elongation of the binding follows: the proton donor is the enolic OH group. Enoli proton participates in the formation of an intramolecular bond.

PLAT772_ALERT_2_B Suspect O-H Bond in CIF: O2' -- H1' .. 1.43 Ang.
Response: Elongation of the binding follows: the proton donor is the enolic OH group. Enoli proton participates in the formation of an intramolecular bond.

PLAT910_ALERT_3_B Missing # of FCF Reflection(s) Below Theta(Min) 20 Note
Response: Some reflections had to be omitted in the refinement for technical reasons.

Complex 1

Table S2. Crystal data and structure refinement for Complex 1.

Identification code	Complex 1
Empirical formula	$C_{24}H_{28}N_2O_4Pd$
Formula weight	514.88
Temperature/K	293(2)
Crystal system	monoclinic
Space group	$P2_1/c$
a/Å	10.7818(15)
b/Å	29.646(4)
c/Å	11.6919(17)
α/°	90
β/°	110.974(16)
γ/°	90
Volume/Å^3	3489.6(9)
Z	6
ρ_{calc}g/cm^3	1.470
μ/mm^{-1}	0.829
F(000)	1584.0
Crystal size/mm^3	0.21 × 0.2 × 0.15
Radiation	MoKα (λ = 0.71073)
2Θ range for data collection/°	8.17 to 50.682
Index ranges	-12 ≤ h ≤ 12, -34 ≤ k ≤ 35, -14 ≤ l ≤ 13
Reflections collected	76403
Independent reflections	6118 [R_{int} = 0.2458, R_{sigma} = 0.1525]
Data/restraints/parameters	6118/0/431
Goodness-of-fit on F^2	1.028
Final R indexes [I>=2σ (I)]	R_1 = 0.0726, wR_2 = 0.1375
Final R indexes [all data]	R_1 = 0.1572, wR_2 = 0.1688
Largest diff. peak/hole / e Å^{-3}	0.94/-0.62

Crystal structure determination of [Complex 1]

Crystal Data for $C_{24}H_{28}N_2O_4Pd$ (*M* =514.88 g/mol): monoclinic, space group $P2_1/c$ (no. 14), *a* = 10.7818(15) Å, *b* = 29.646(4) Å, *c* = 11.6919(17) Å, *β* = 110.974(16)°, *V* = 3489.6(9) Å^3, *Z* = 6, *T* = 293(2) K, μ(MoKα) = 0.829 mm^{-1}, *Dcalc* = 1.470 g/cm^3, 76403 reflections measured (8.17° ≤ 2Θ ≤ 50.682°), 6118 unique (R_{int} = 0.2458, R_{sigma} = 0.1525) which were used in all calculations. The final R_1 was 0.0726 (I > 2σ(I)) and wR_2 was 0.1688 (all data).

CheckCif alert is listed according to Alert Level B for compound complex 1

RINTA01_ALERT_3_B The value of Rint is greater than 0.18 Rint given 0.246
PLAT020_ALERT_3_B The value of Rint is greater than 0.12 ..... 0.246 Report

Response: Crystals diffracted extremely weakly. Multiple attempts were made to grow better diffracting crystals. All results were consistent with the model in this report, however, all yielded serious problems due to weak diffraction and disorder in the atom positions.

The Crystal quality was not good. After several attempts of data collection, there ported one is found to be the best one.

PLAT201_ALERT_2_B Isotropic non-H Atoms in Main Residue(s) ..... 3 Report
Response: These are atoms of an unordered tert-butyl group, divided into two positions. Disordered carbon atoms in the tert-butyl group were refined by using isotropic displacement parameters.

PLAT910_ALERT_3_B Missing # of FCF Reflection(s) Below Theta(Min) 29 Note
Response: Some reflections had to be omitted in the refinement for technical reasons.

Complex 3

Table S3. Crystal data and structure refinement for Complex 3.

Identification code	Complex 3
Empirical formula	$C_{49}H_{62}Cl_2N_6O_{14}Pd$
Formula weight	1136.34
Temperature/K	293(2)
Crystal system	monoclinic
Space group	I2/a
a/Å	16.2535(4)
b/Å	10.2732(3)
c/Å	32.8746(8)
α/°	90
β/°	94.198(2)
γ/°	90
Volume/Å^3	5474.5(2)
Z	4
ρ_{calc}g/cm^3	1.379
μ/mm^{-1}	0.503
F(000)	2360.0
Crystal size/mm^3	0.2 × 0.15 × 0.1
Radiation	MoKα (λ = 0.71073)
2Θ range for data collection/°	8.316 to 50.664
Index ranges	-19 ≤ h ≤ 19, -12 ≤ k ≤ 12, -38 ≤ l ≤ 39
Reflections collected	106301
Independent reflections	4820 [R_{int} = 0.1420, R_{sigma} = 0.0670]
Data/restraints/parameters	4820/0/364
Goodness-of-fit on F^2	1.070
Final R indexes [I>=2σ (I)]	R_1 = 0.0532, wR_2 = 0.1242
Final R indexes [all data]	R_1 = 0.0957, wR_2 = 0.1414
Largest diff. peak/hole / e Å^{-3}	0.86/-0.39

Crystal structure determination of [Complex 3]

Crystal Data for $C_{49}H_{62}Cl_2N_6O_{14}Pd$ (M =1136.34 g/mol): monoclinic, space group I2/a (no. 15), a = 16.2535(4) Å, b = 10.2732(3) Å, c = 32.8746(8) Å, β = 94.198(2)°, V = 5474.5(2) Å^3, Z = 4, T = 293(2) K, μ(MoKα) = 0.503 mm^{-1}, *Dcalc* = 1.379 g/cm^3, 106301 reflections measured (8.316° ≤ 2Θ ≤ 50.664°), 4820 unique (R_{int} = 0.1420, R_{sigma} = 0.0670) which were used in all calculations. The final R_1 was 0.0532 (I > 2σ(I)) and wR_2 was 0.1414 (all data).

CheckCif alert is listed according to Alert Level B for compound complex 3

PLAT242_ALERT_2_B Low 'MainMol' Ueq as Compared to Neighbors of C9 Check
PLAT242_ALERT_2_B Low 'MainMol' Ueq as Compared to Neighbors of C9' Check
Response: These are carbon atoms derived from the terminal tert-butyl group.
PLAT910_ALERT_3_B Missing # of FCF Reflection(s) Below Theta(Min) 21 Note

Response: Some reflections had to be omitted in the refinement for technical reasons.

Complex 4

Table S4. Crystal data and structure refinement for Complex 4.

Identification code	**Complex 4**
Empirical formula	$C_{48}H_{64}N_6O_{16}Pd$
Formula weight	1087.45
Temperature/K	293(2)
Crystal system	monoclinic
Space group	C2/c
a/Å	12.4086(3)
b/Å	16.0277(4)
c/Å	26.8245(7)
α/°	90
β/°	91.931(2)
γ/°	90
Volume/Å^3	5331.9(2)
Z	4
ρ_{calc}g/cm^3	1.355
μ/mm^{-1}	0.419
F(000)	2272.0
Crystal size/mm^3	0.3 × 0.2 × 0.15
Radiation	MoKα (λ = 0.71073)
2Θ range for data collection/°	8.306 to 50.692
Index ranges	-14 ≤ h ≤ 14, -19 ≤ k ≤ 19, -32 ≤ l ≤ 31
Reflections collected	92107
Independent reflections	4691 [R_{int} = 0.1011, R_{sigma} = 0.0498]
Data/restraints/parameters	4691/0/405
Goodness-of-fit on F^2	1.047
Final R indexes [I>=2σ (I)]	R_1 = 0.0541, wR_2 = 0.1269
Final R indexes [all data]	R_1 = 0.0951, wR_2 = 0.1463
Largest diff. peak/hole / e Å^{-3}	0.48/-0.39

Crystal structure determination of [Complex 4]

Crystal Data for $C_{48}H_{64}N_6O_{16}Pd$ (M =1087.45 g/mol): monoclinic, space group C2/c (no. 15), a = 12.4086(3) Å, b = 16.0277(4) Å, c = 26.8245(7) Å, β = 91.931(2)°, V = 5331.9(2) Å^3, Z = 4, T = 293(2) K, μ(MoKα) = 0.419 mm^{-1}, $Dcalc$ = 1.355 g/cm^3, 92107 reflections measured (8.306° ≤ 2Θ ≤ 50.692°), 4691 unique (R_{int} = 0.1011, R_{sigma} = 0.0498) which were used in all calculations. The final R_1 was 0.0541 (I > 2σ(I)) and wR_2 was 0.1463 (all data).

CheckCif alert is listed according to Alert Level B for compound complex 4

PLAT221_ALERT_2_B Solv./Anion Resd 2 N Ueq(max)/Ueq(min) Range 9.7 Ratio
PLAT234_ALERT_4_B Large Hirshfeld Difference C9' -- C12' .. 0.30 Ang.
Response: The Crystal quality was not good.

PLAT242_ALERT_2_B Low 'MainMol' Ueq as Compared to Neighbors of C9 Check
PLAT242_ALERT_2_B Low 'MainMol' Ueq as Compared to Neighbors of C9' Check
Response: These are carbon atoms derived from the terminal tert-butyl group.

PLAT306_ALERT_2_B Isolated Oxygen Atom (H-atoms Missing ?) ..... O5 Check

PLAT910_ALERT_3_B Missing # of FCF Reflection(s) Below Theta(Min) 19 Note
Response: Some reflections had to be omitted in the refinement for technical reasons.

3. Acid-base switching

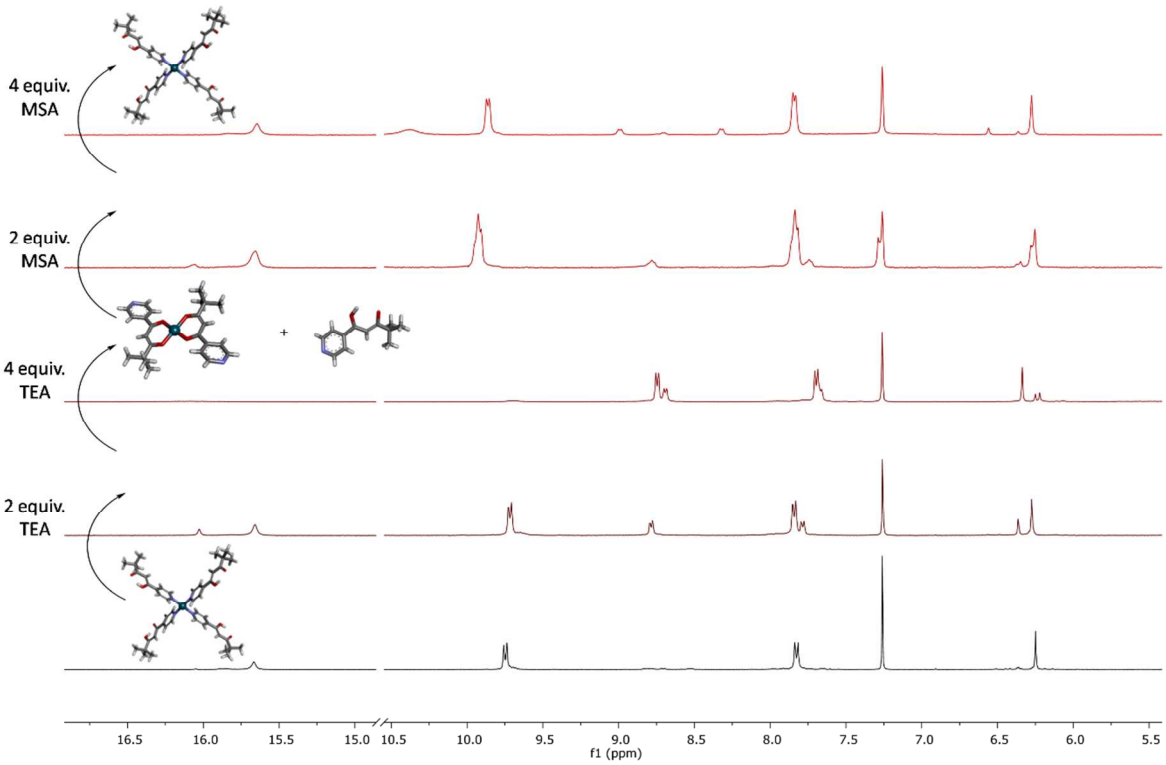

Figure S16. ^{1}H NMR (300 MHz, $CDCl_3$) acid-base titration spectra showing the reversible structural switching between the complexes **3** and **1** in $CDCl_3$.

4. GC-MS analysis for Suzuki-Miyaura Cross Coupling Reactions

4.1. For complex 1

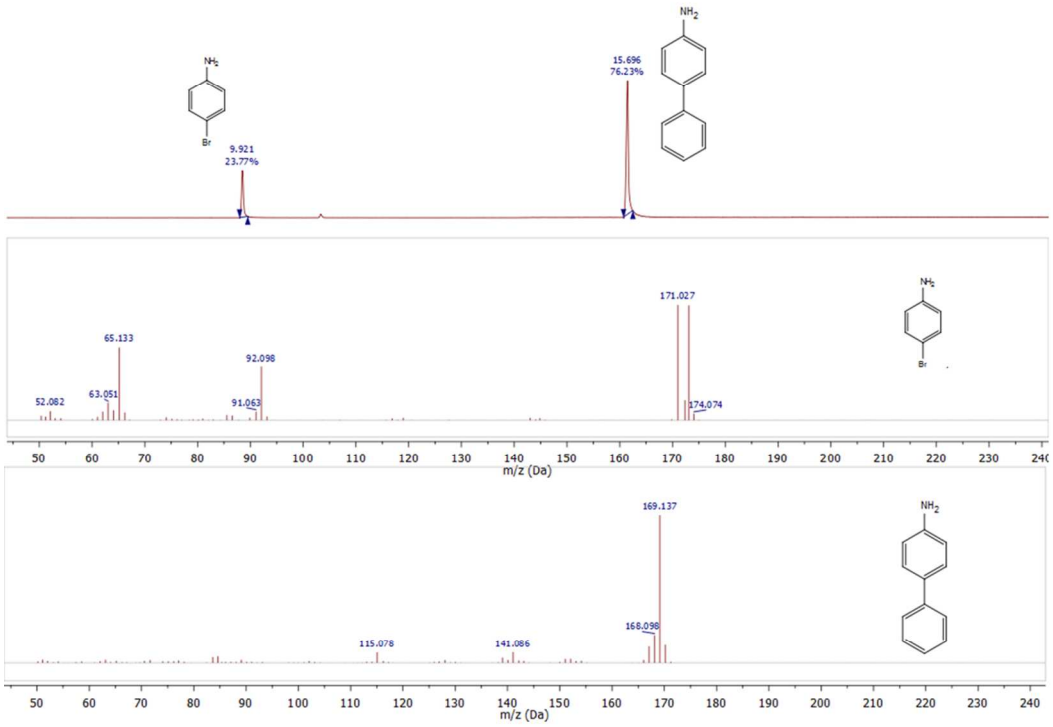

Figure S17. GC-MS chromatogram showing the conversion of 4-bromoaniline.

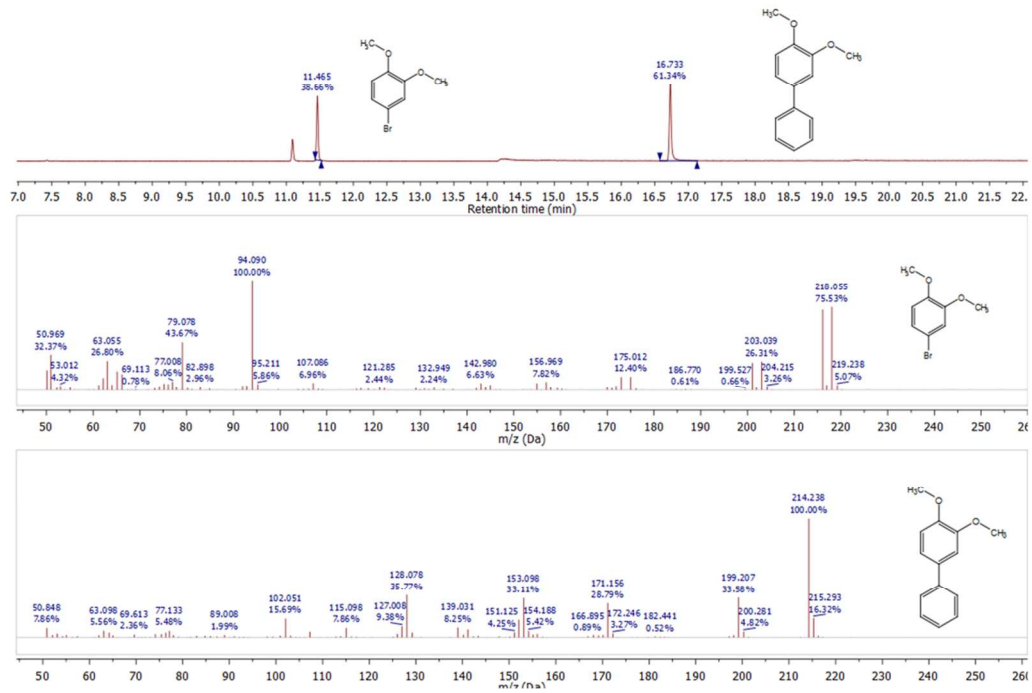

Figure S18. GC-MS chromatogram showing the conversion of 4-bromoveratrole.

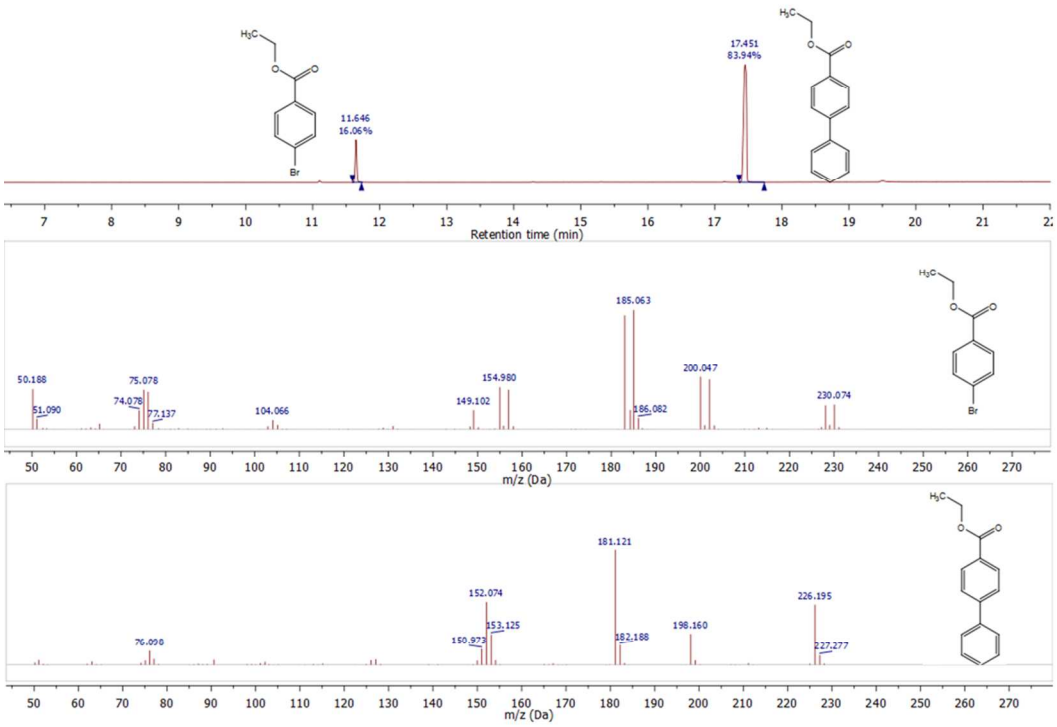

Figure S19. GC-MS chromatogram showing the conversion of ethyl 4-bromobenzoate.

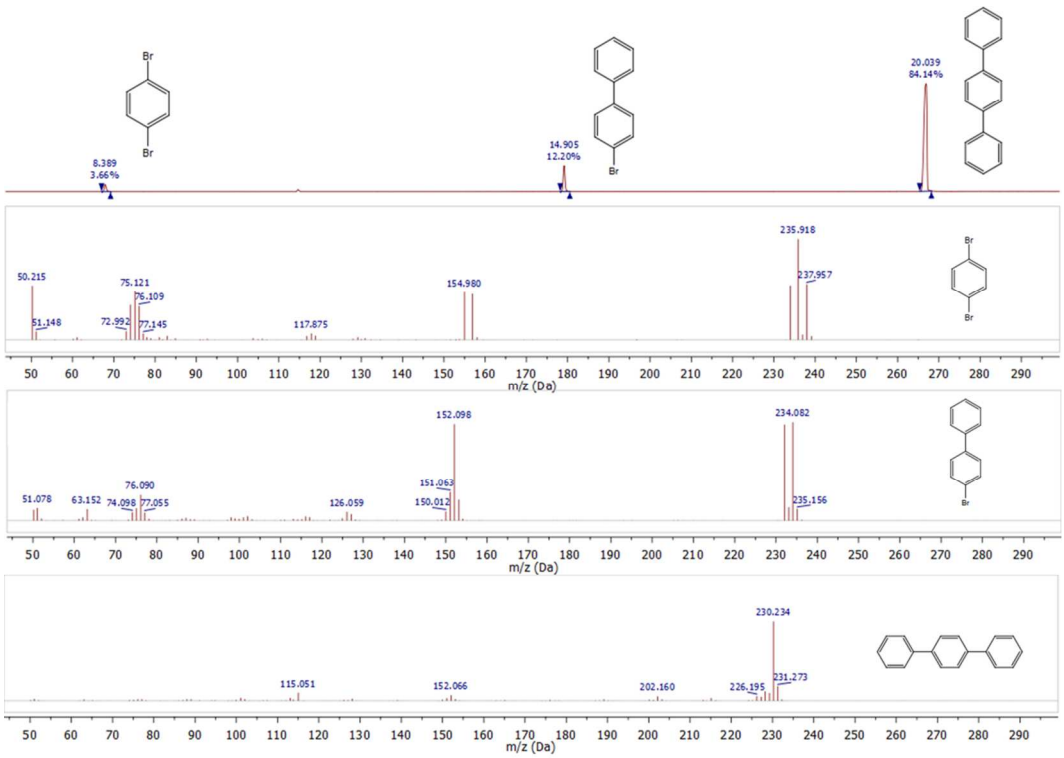

Figure S20. GC-MS chromatogram showing the conversion of 1,4-dibromobenzene.

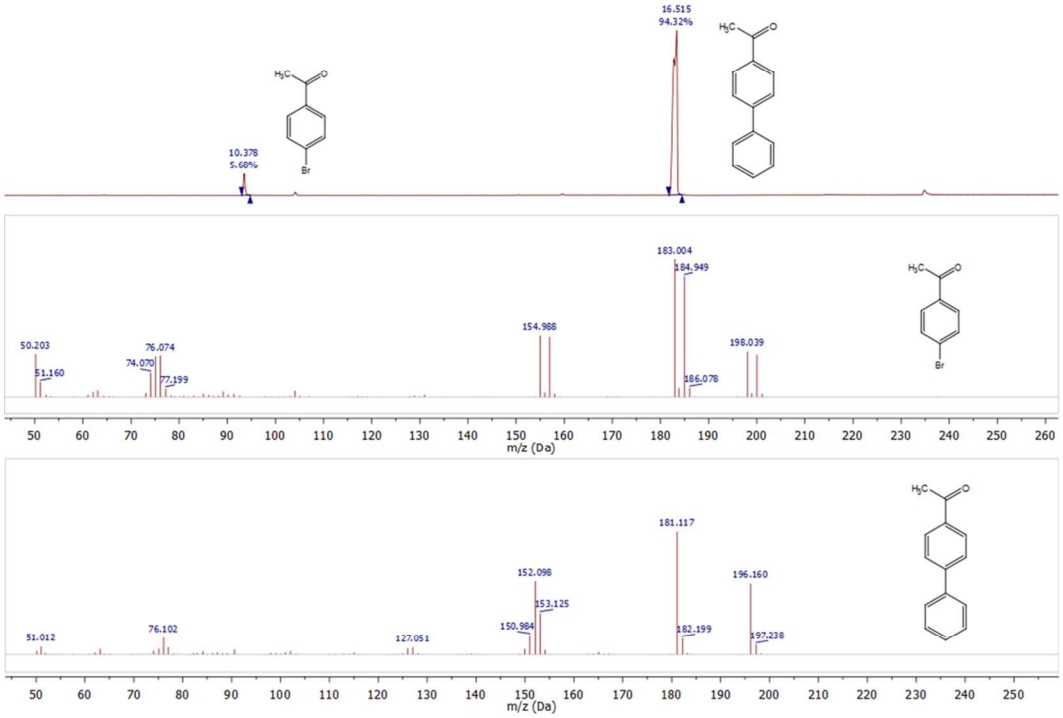

Figure S21. GC-MS chromatogram showing the conversion of 4'-bromoacetophenone.

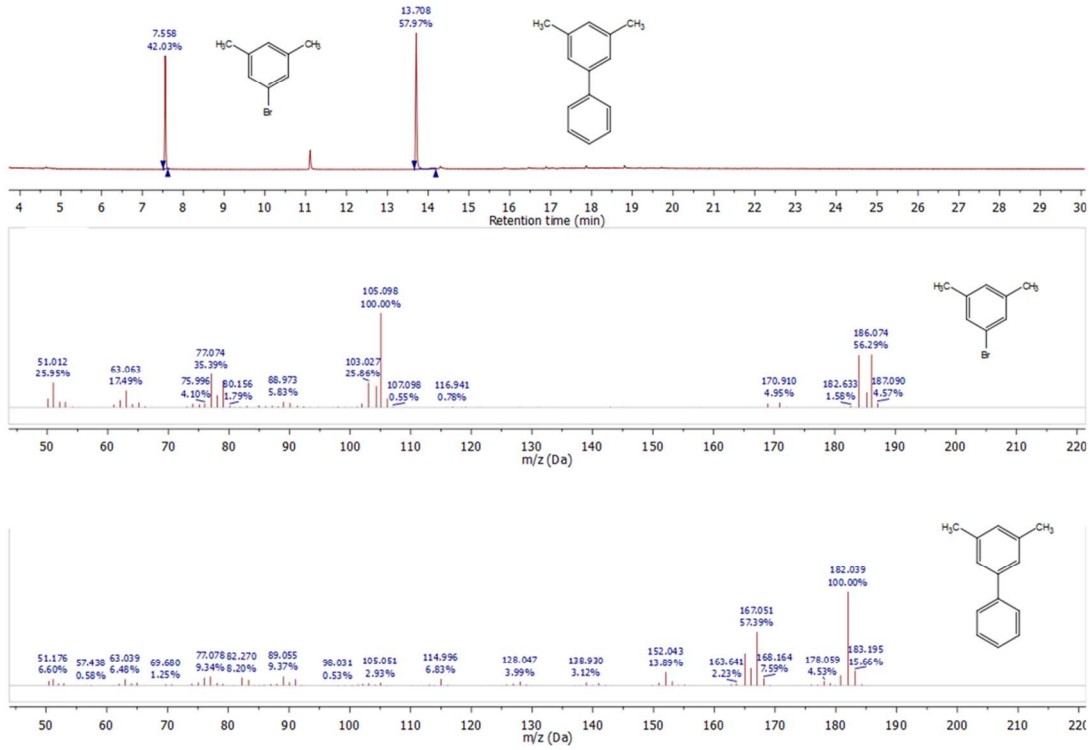

Figure S22. GC-MS chromatogram showing the conversion of 1-bromo-3,5-dimethylbenzene.

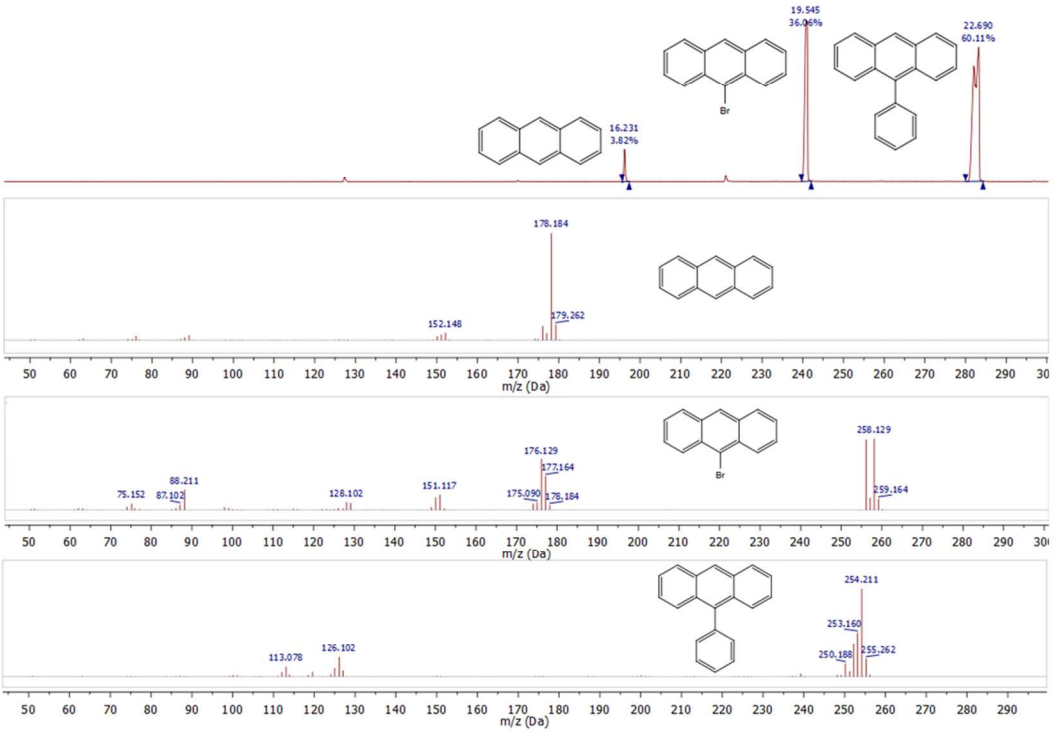

Figure S23. GC-MS chromatogram showing the conversion of 9-bromoanthracene.

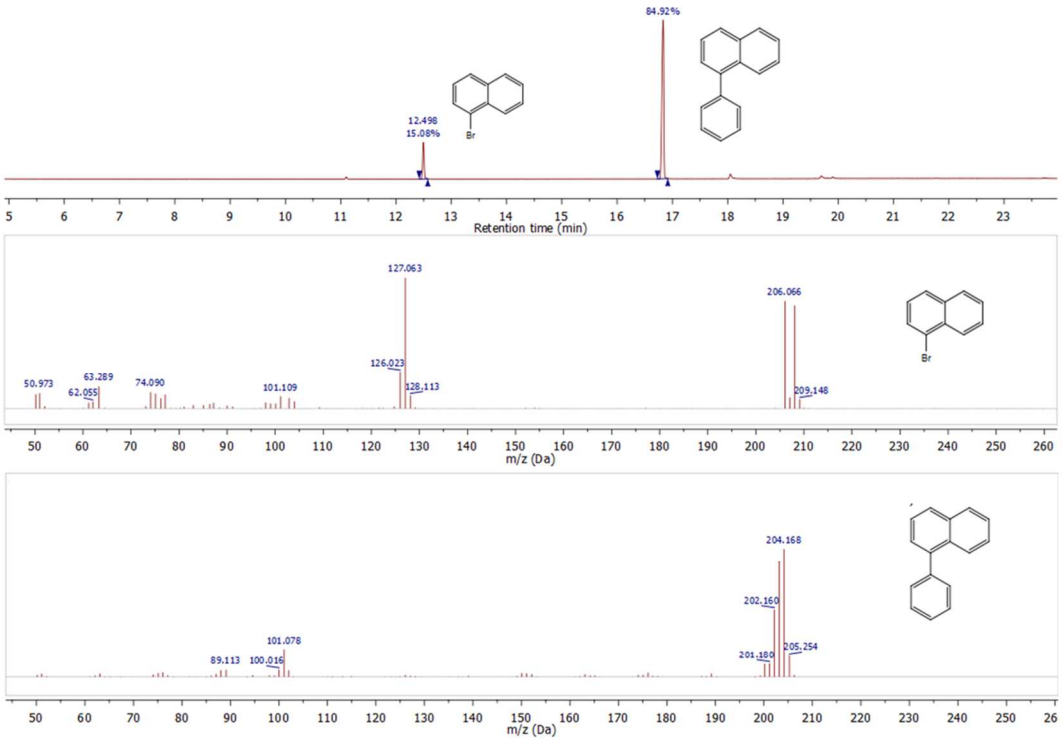

Figure S24. GC-MS chromatogram showing the conversion of 1-bromonaphthalene.

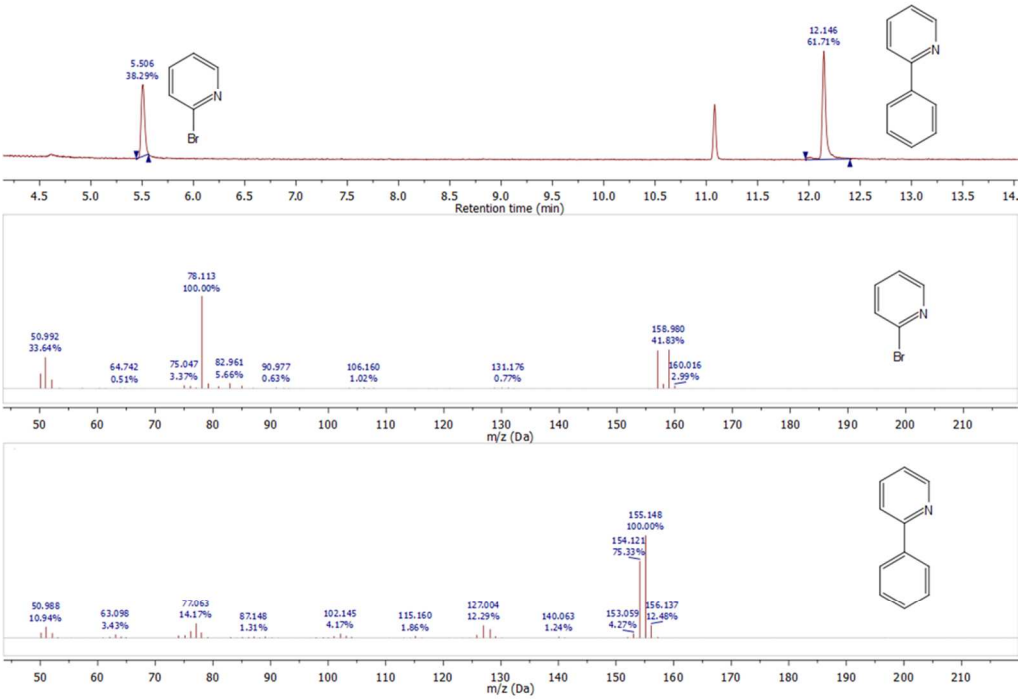

Figure S25. GC-MS chromatogram showing the conversion of 2-bromopyridine.

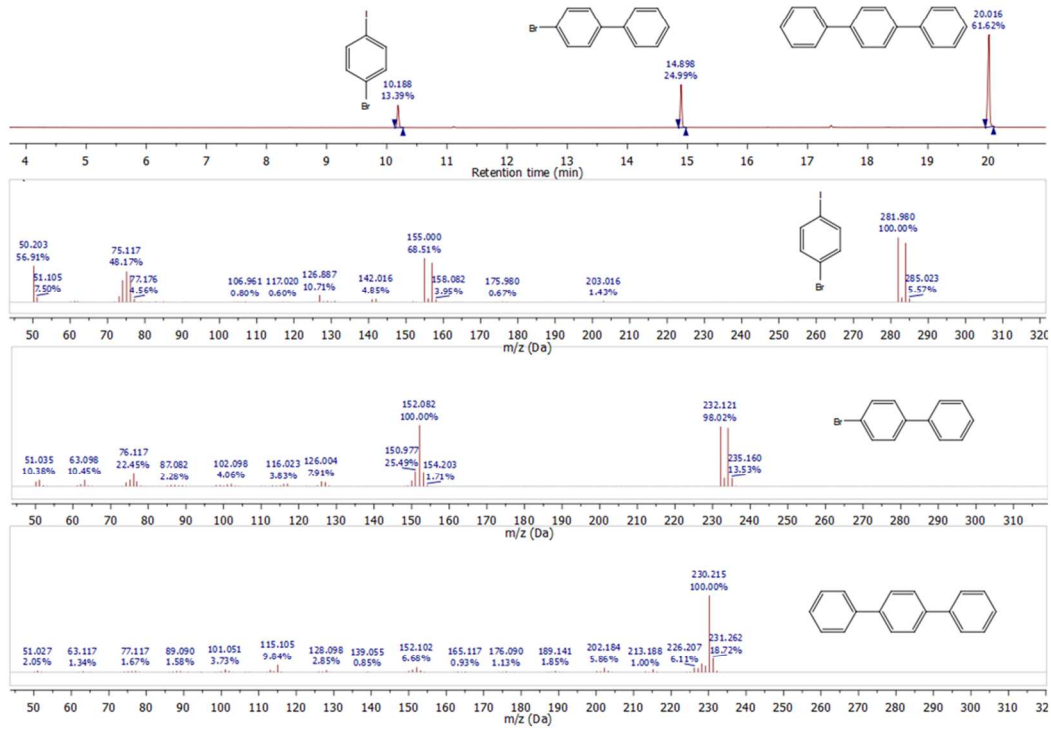

Figure S26. GC-MS chromatogram showing the conversion of 1-bromo-4-iodobenzene.

4.2. For complex 2

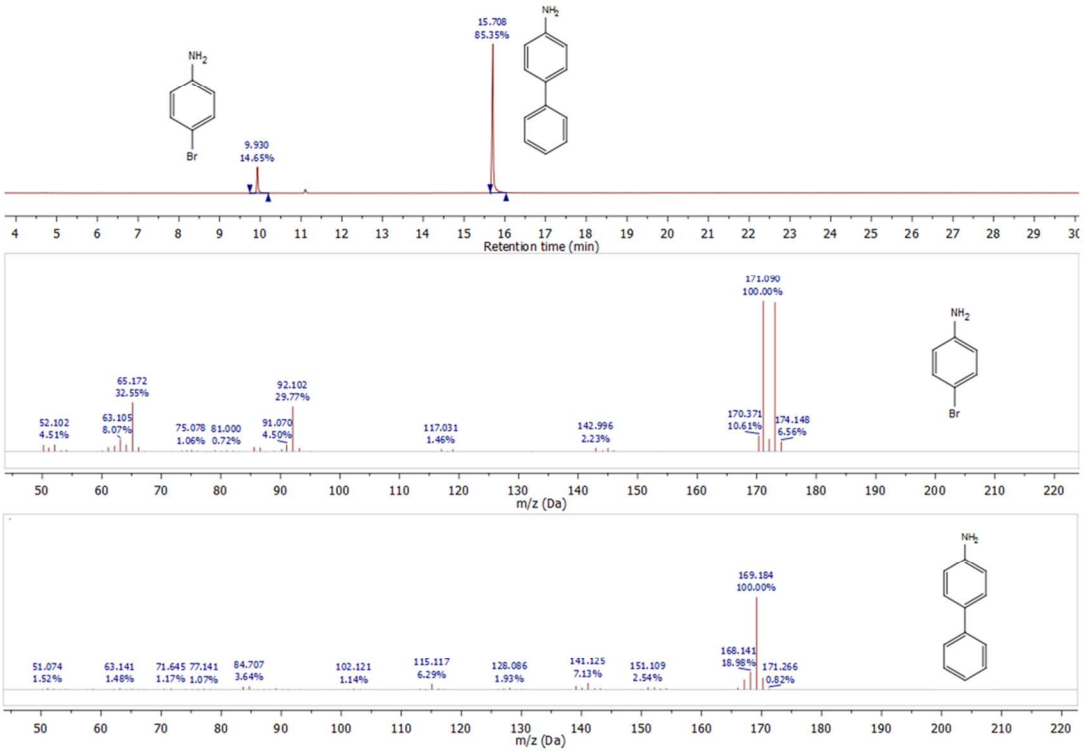

Figure S27. GC-MS chromatogram showing the conversion of 4-bromoaniline.

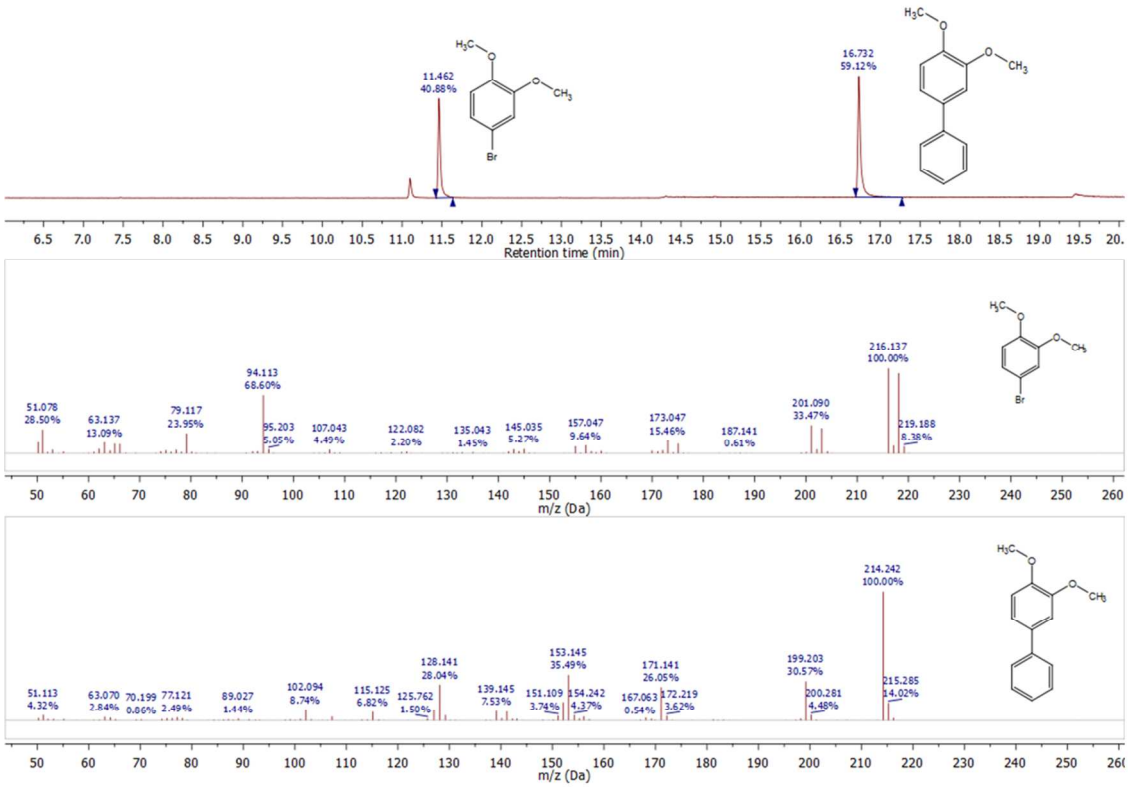

Figure S28. GC-MS chromatogram showing the conversion of 4-bromoveratrole.

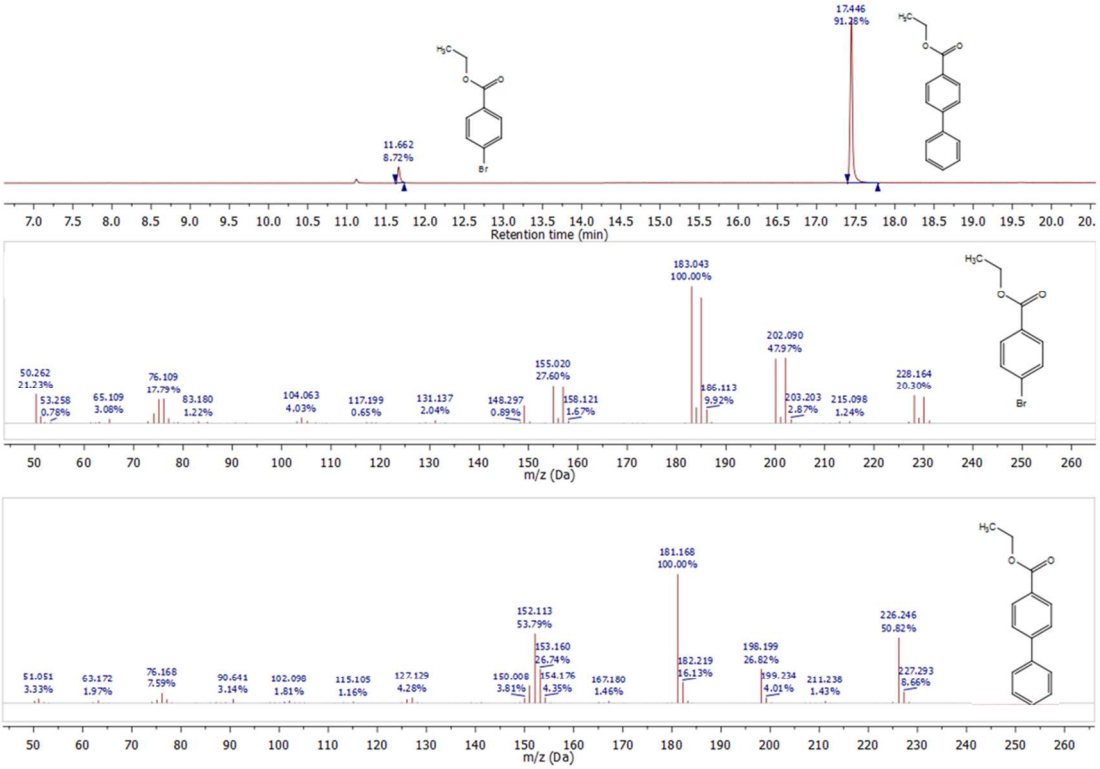

Figure S29. GC-MS chromatogram showing the conversion of and ethyl 4-bromobenzoate.

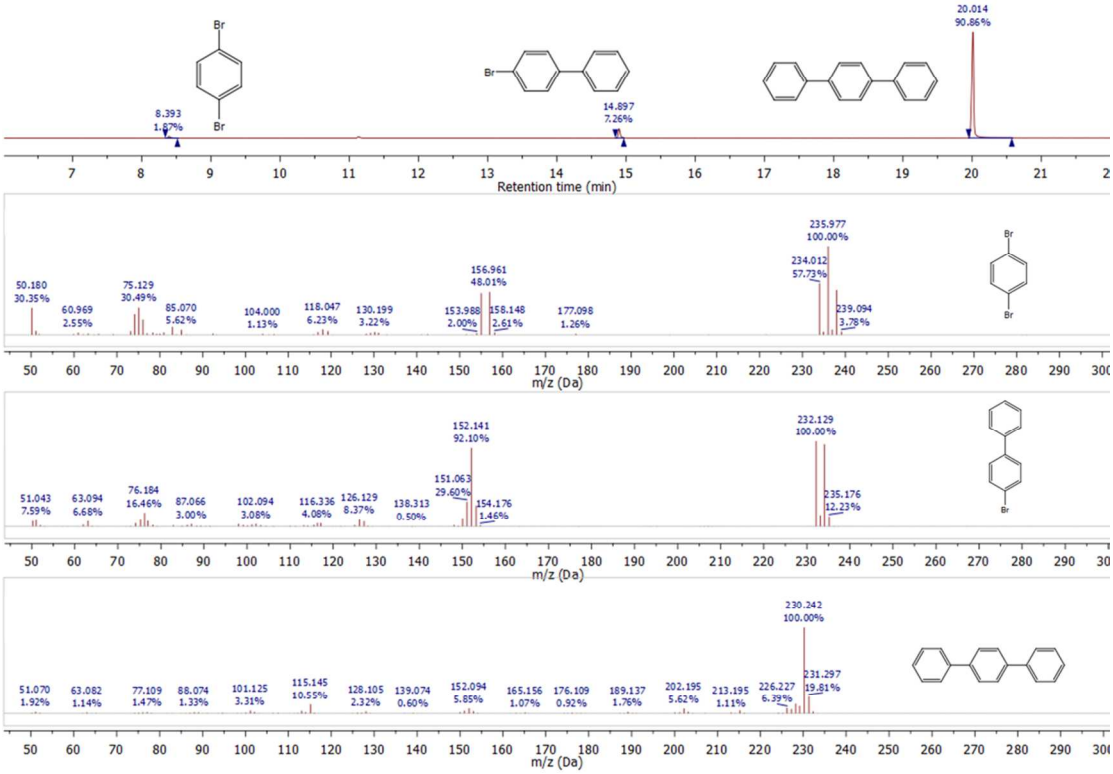

Figure S30. GC-MS chromatogram showing the conversion of 1,4-dibromobenzene.

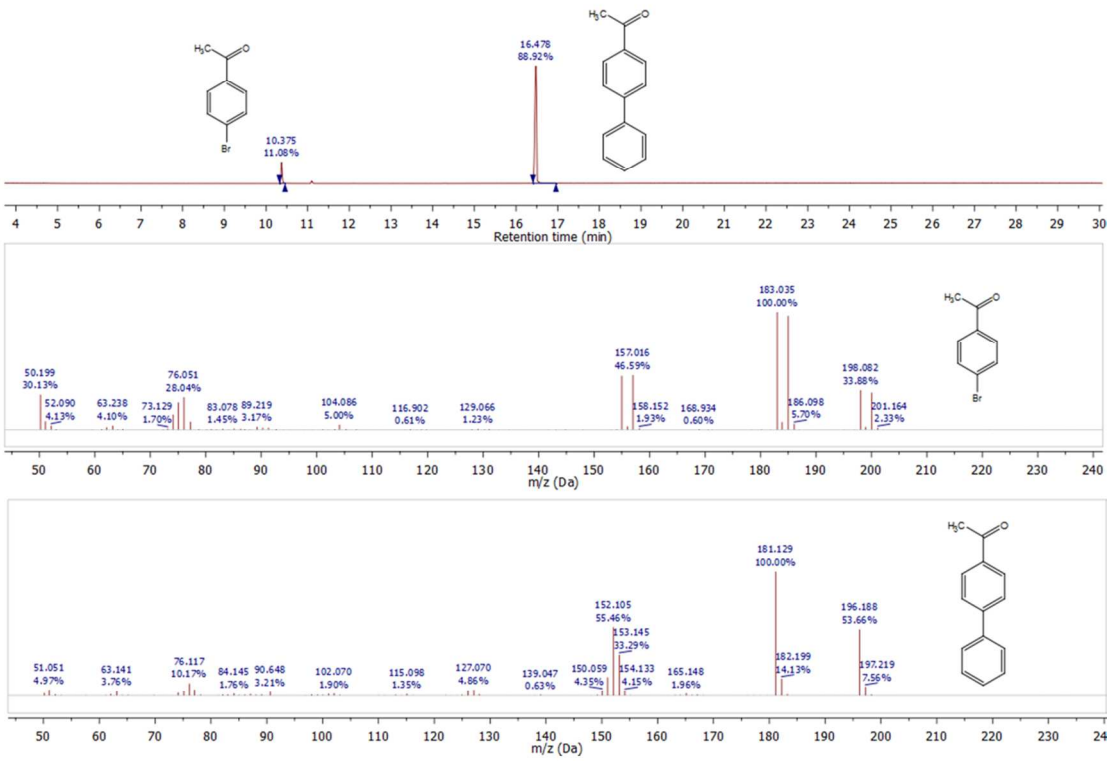

Figure S31. GC-MS chromatogram showing the conversion of 4'-bromoacetophenone.

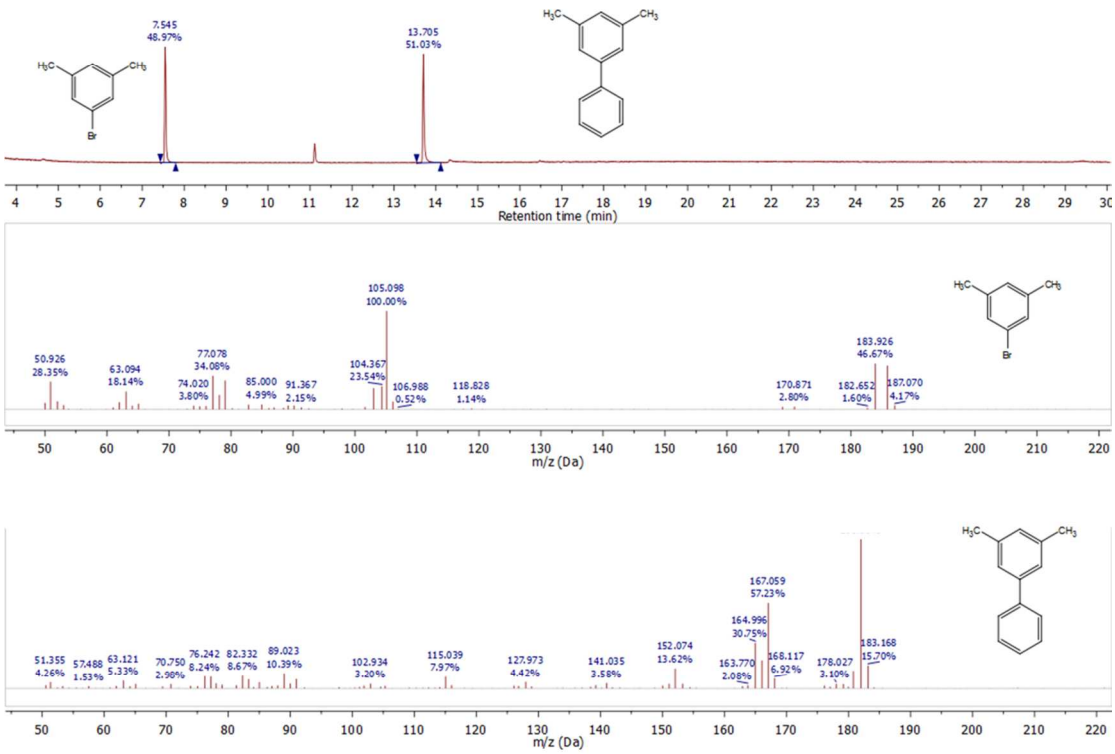

Figure S32. GC-MS chromatogram showing the conversion of 1-bromo-3,5-dimethylbenzene.

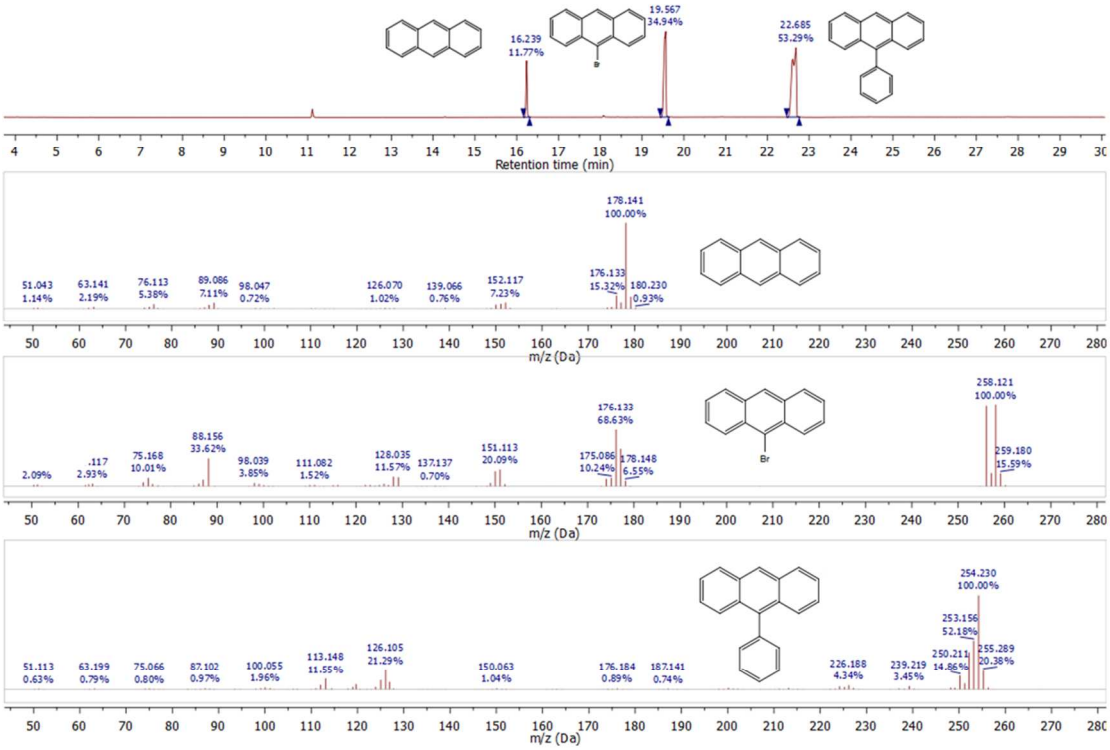

Figure S33. GC-MS chromatogram showing the conversion of 9-bromoanthracene.

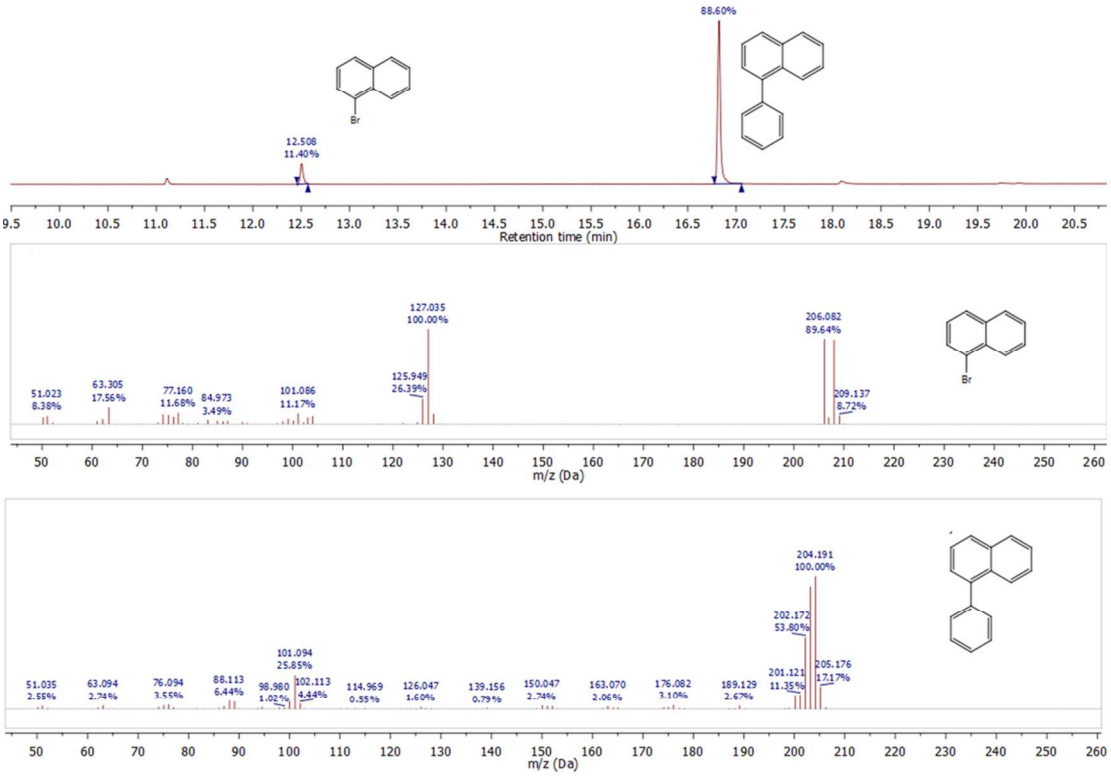

Figure S34. GC-MS chromatogram showing the conversion of 1-bromonaphthalene.

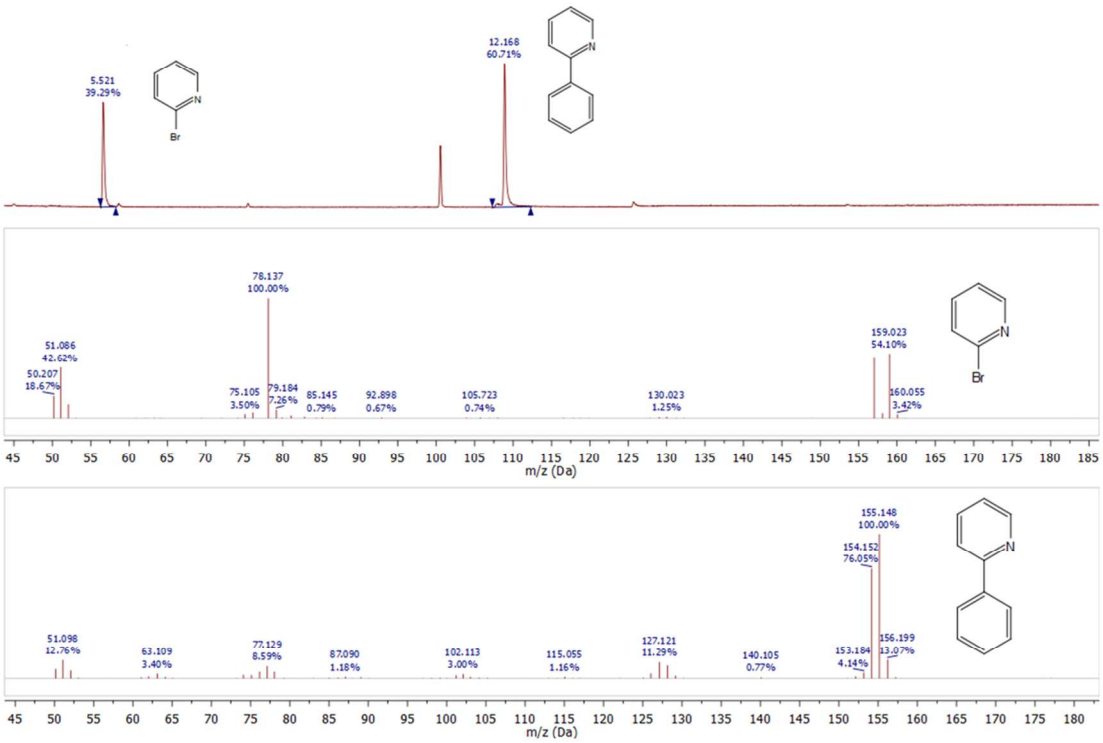

Figure S35. GC-MS chromatogram showing the conversion of 2-bromopyridine.

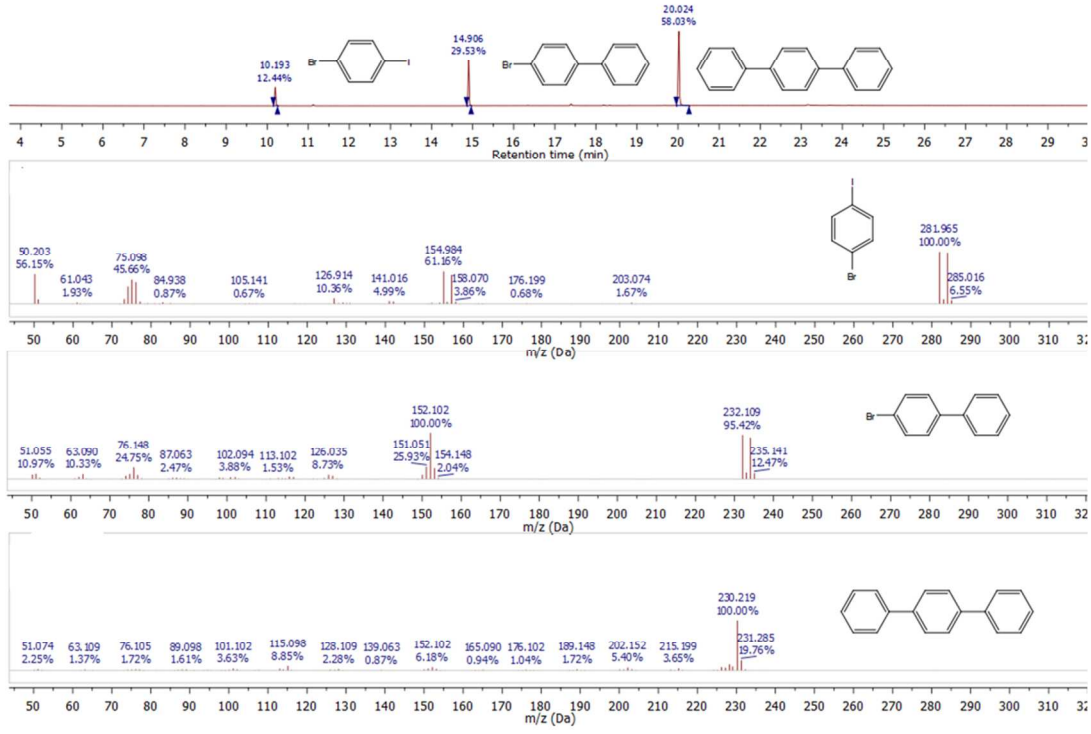

Figure S36. GC-MS chromatogram showing the conversion of 1-bromo-4-iodobenzene.

4.3. Catalytic activity of catalyst $Pd(OAc)_2$, $Pd(acac)_2$ and $Pd(PPh_3)_2Cl_2$ in the reactions conditions used for 1 and 2 and degradation $[Pd(Py)_4](NO_3)_2$ under the influence of base

a) degradation $[Pd(Py)_4](NO_3)_2$ under the influence of base.

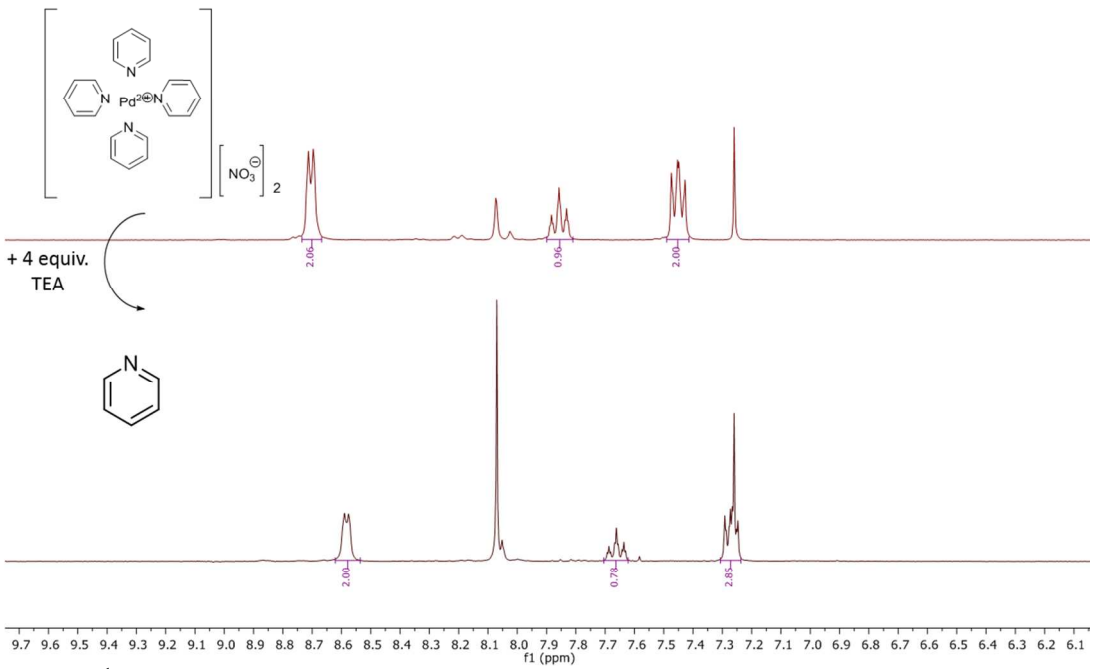

Figure S37. ^{1}H NMR (300 MHz, $CDCl_3$) base titration spectra showing degradation of the complexes **$[Pd(Py)_4](NO_3)_2$** to free pyridine in $CDCl_3$.

b) $Pd(OAc)_2$ (0.01 mol %) + 0.02 mol % of ligand

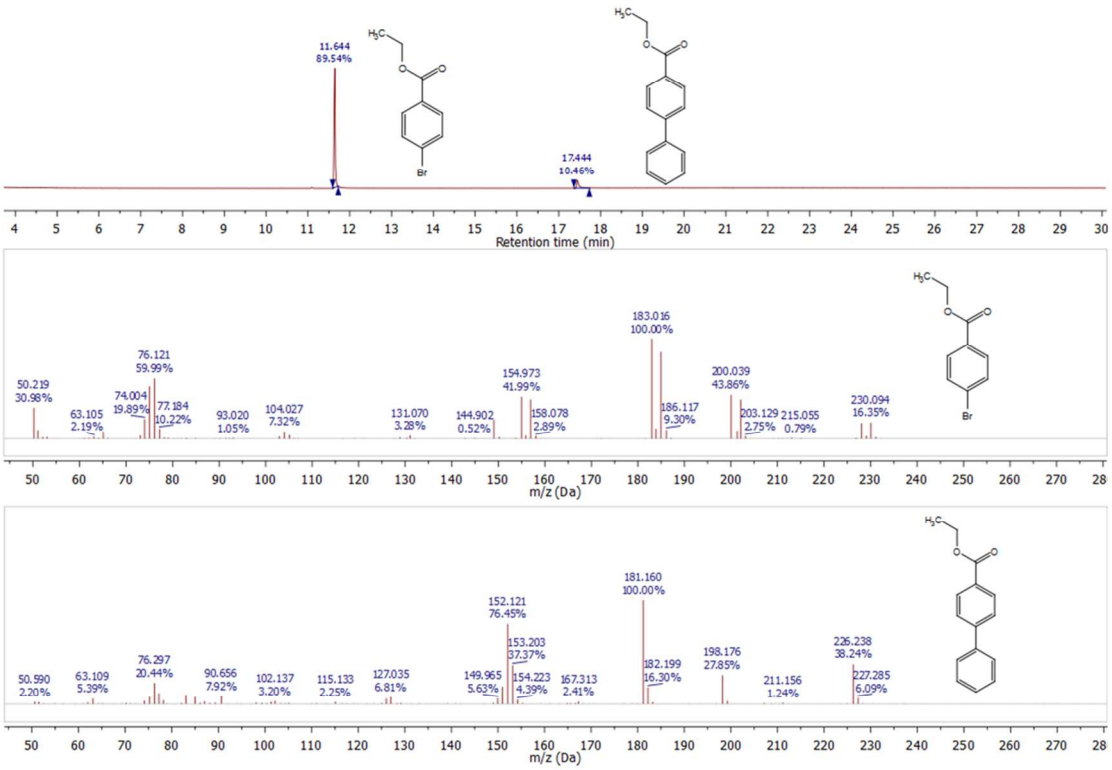

Figure S38. GC-MS chromatogram showing the conversion of and ethyl 4-bromobenzoate for catalyst $Pd(OAc)_2$ (0.01 mol %).

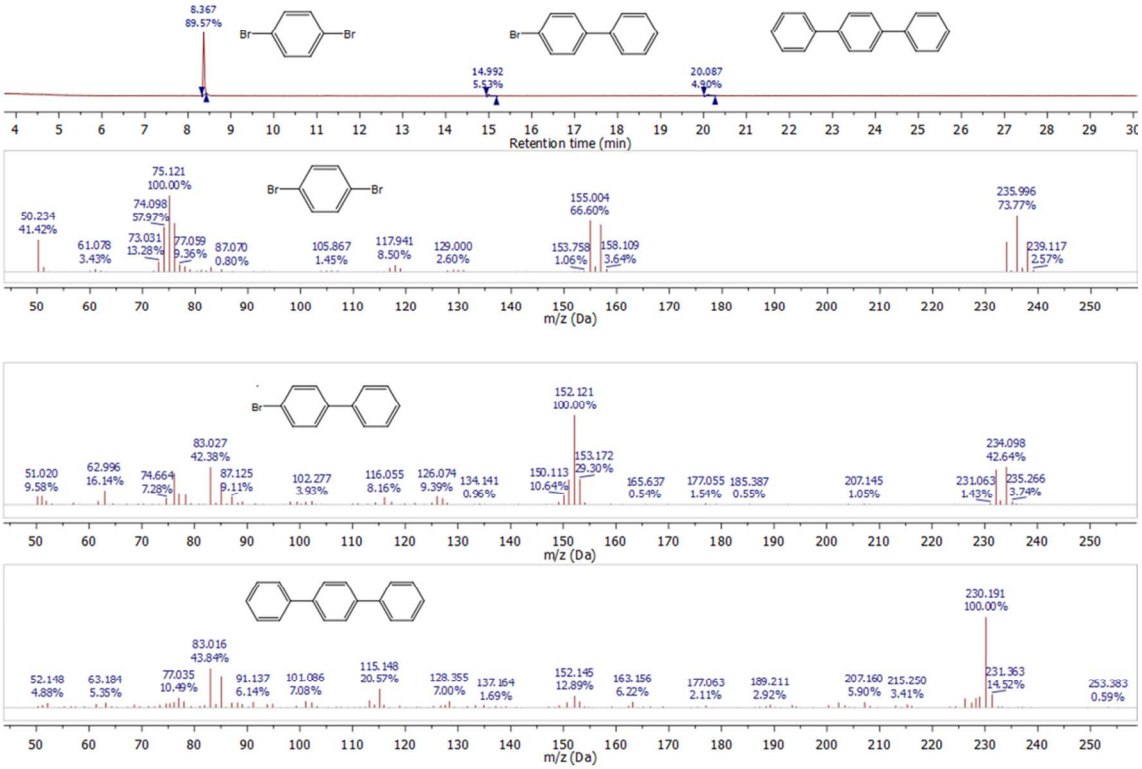

Figure S39. GC-MS chromatogram showing the conversion of 1,4-dibromobenzene for catalyst $Pd(OAc)_2$ (0.01 mol %).

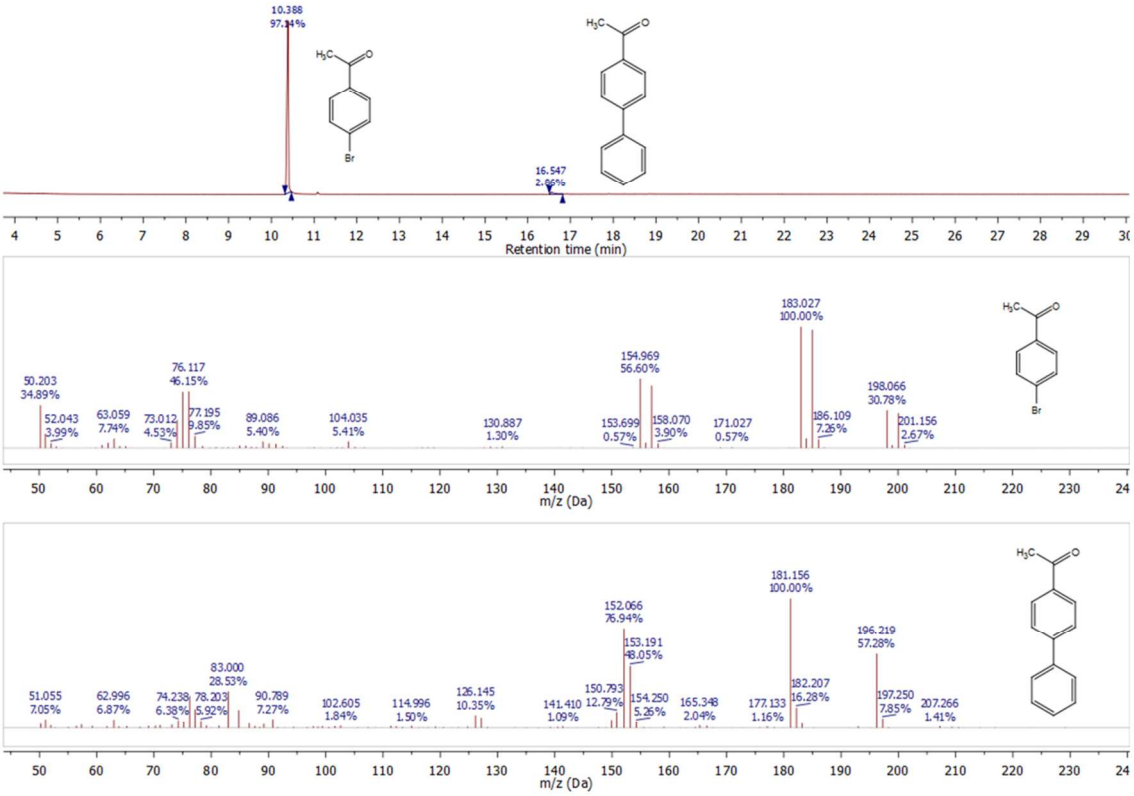

Figure S40. GC-MS chromatogram showing the conversion of 4'-bromoacetophenone for catalyst $Pd(OAc)_2$ (0.01 mol %).

c) $Pd(OAc)_2$ (1 mol %) + 4 mol % of ligand

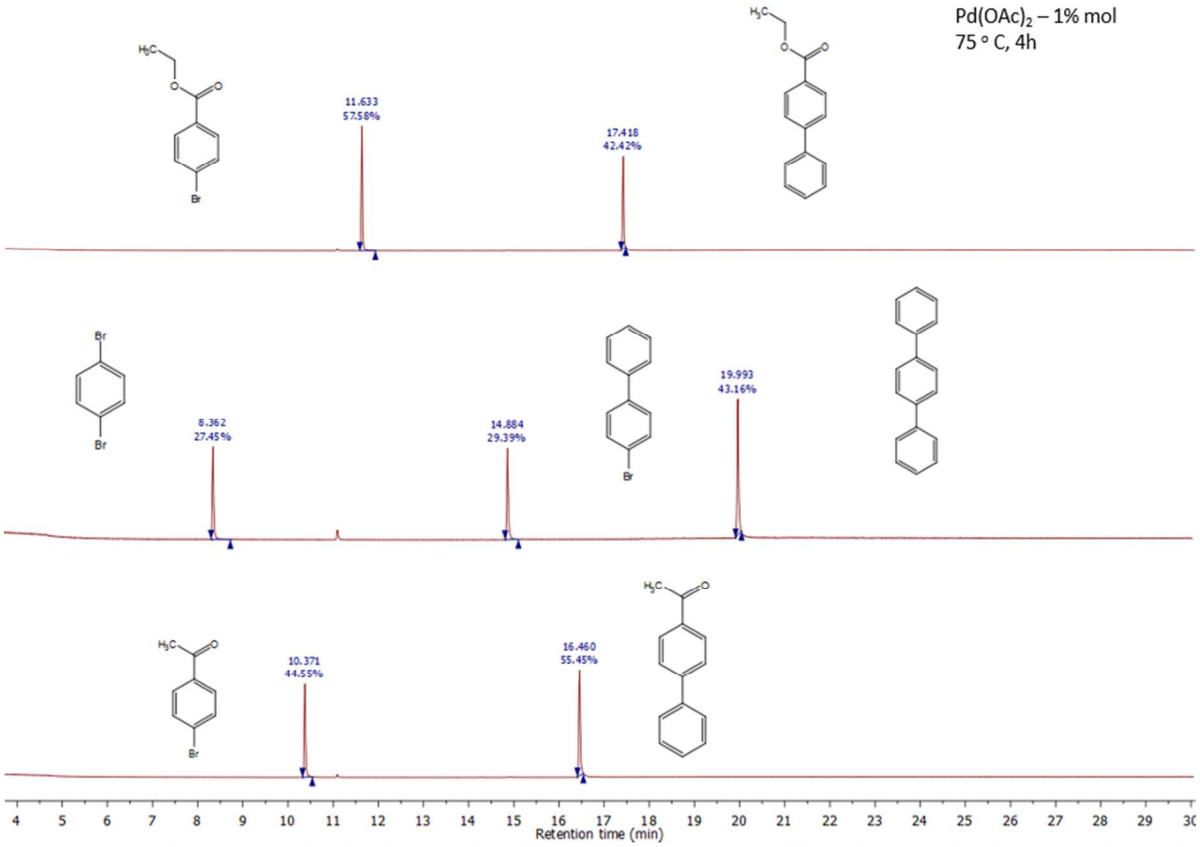

Figure S41. GC chromatograms showing the conversion of ethyl 4-bromobenzoate, 1,4-dibromobenzene and 4'-bromoacetophenone for catalyst $Pd(OAc)_2$ (1 mol %).

d) $Pd(acac)_2$ (0.01 mol %)

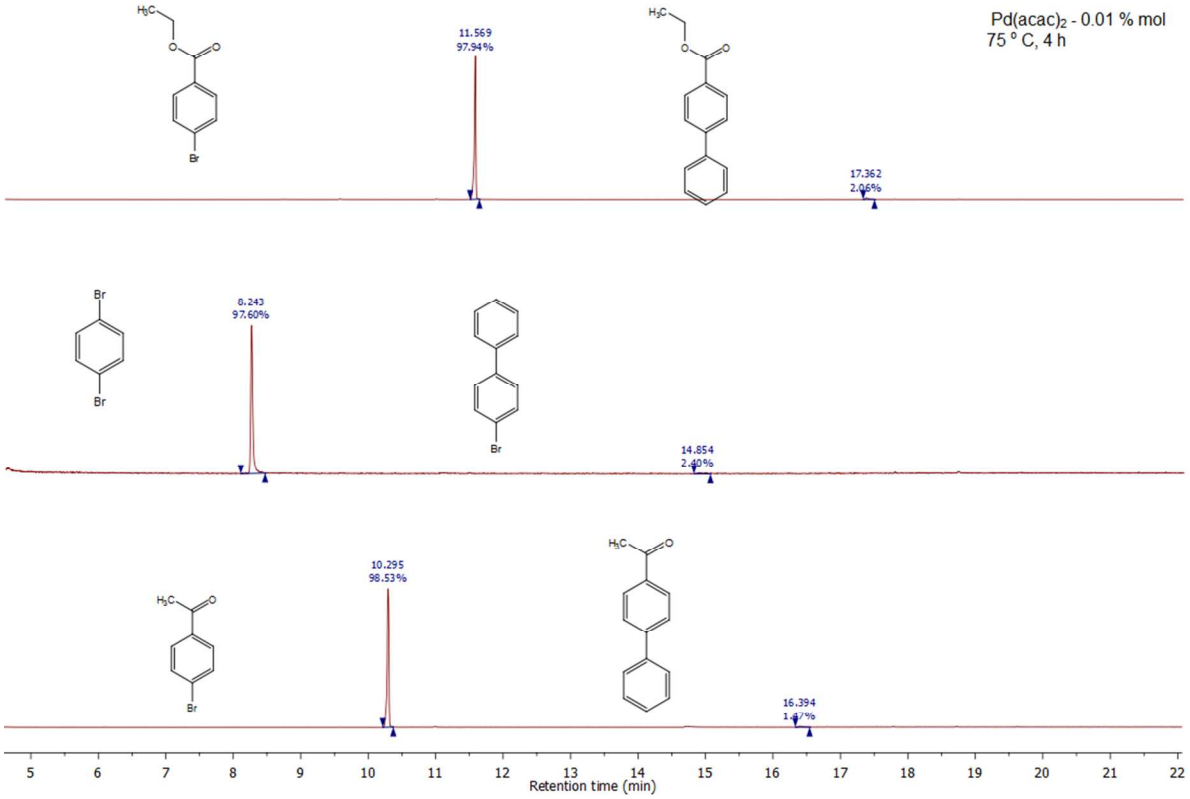

Figure S42. GC chromatograms showing the conversion of ethyl 4-bromobenzoate, 1,4-dibromobenzene and 4'-bromoacetophenone for catalyst $Pd(acac)_2$ (0.01 mol %).

e) $Pd(acac)_2$ (1 mol %)

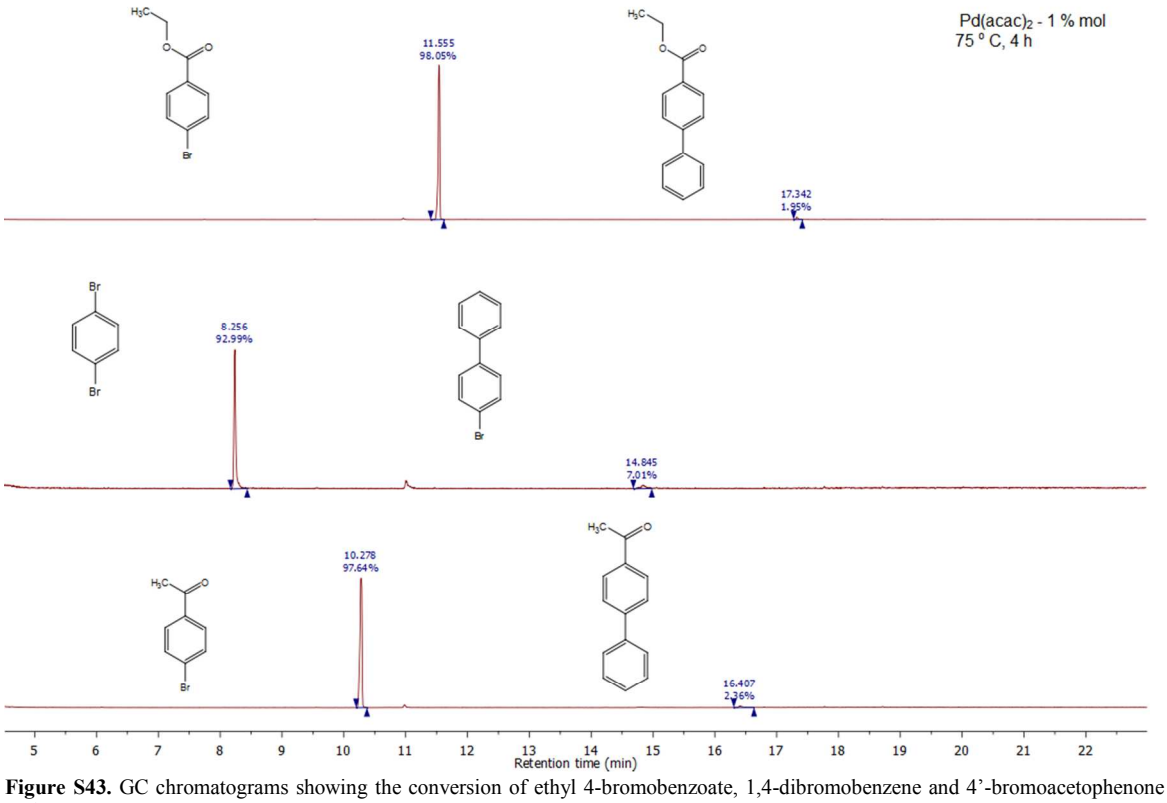

Figure S43. GC chromatograms showing the conversion of ethyl 4-bromobenzoate, 1,4-dibromobenzene and 4'-bromoacetophenone for catalyst $Pd(acac)_2$ (1 mol %).

f) $Pd(PPh_3)_2Cl_2$ (0.01 mol %)

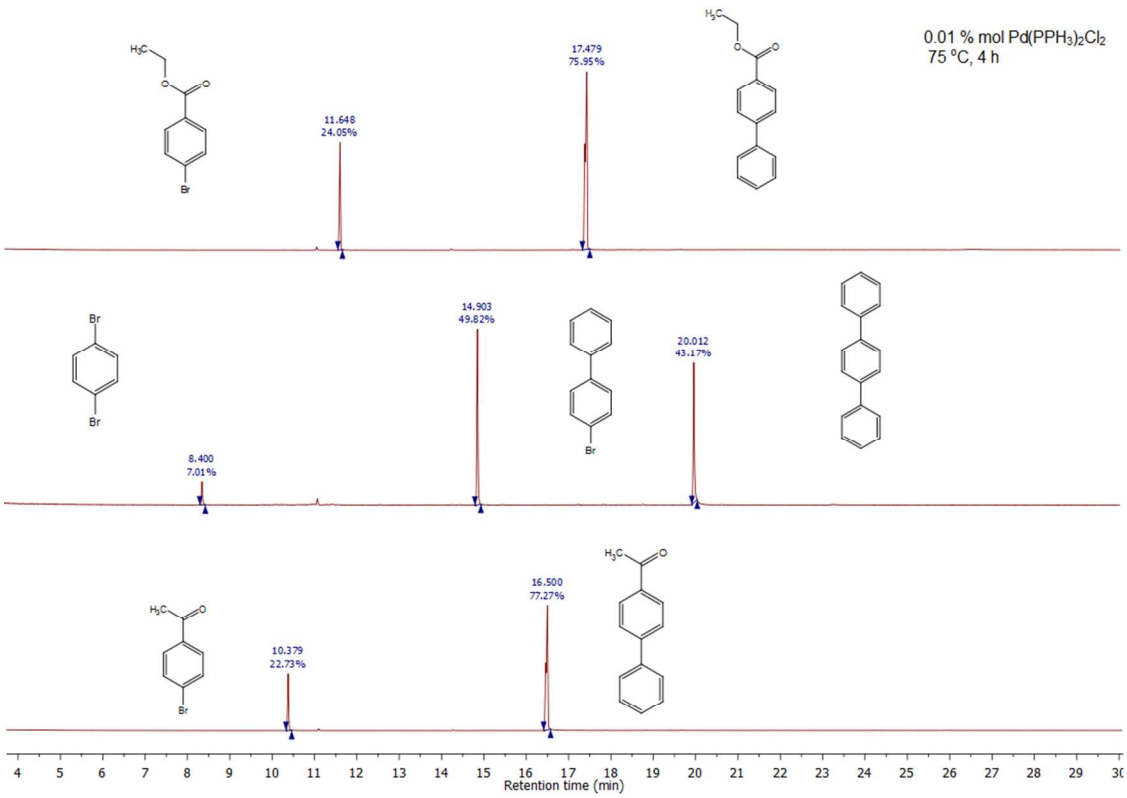

Figure S44. GC chromatograms showing the conversion of ethyl 4-bromobenzoate, 1,4-dibromobenzene and 4'-bromoacetophenone for catalyst $Pd(PPh_3)_2Cl_2$ (0.01 mol %).

Acid-base on/off experiment with $Pd(OAc)_2$, bromo aryl and phenylboronic acid

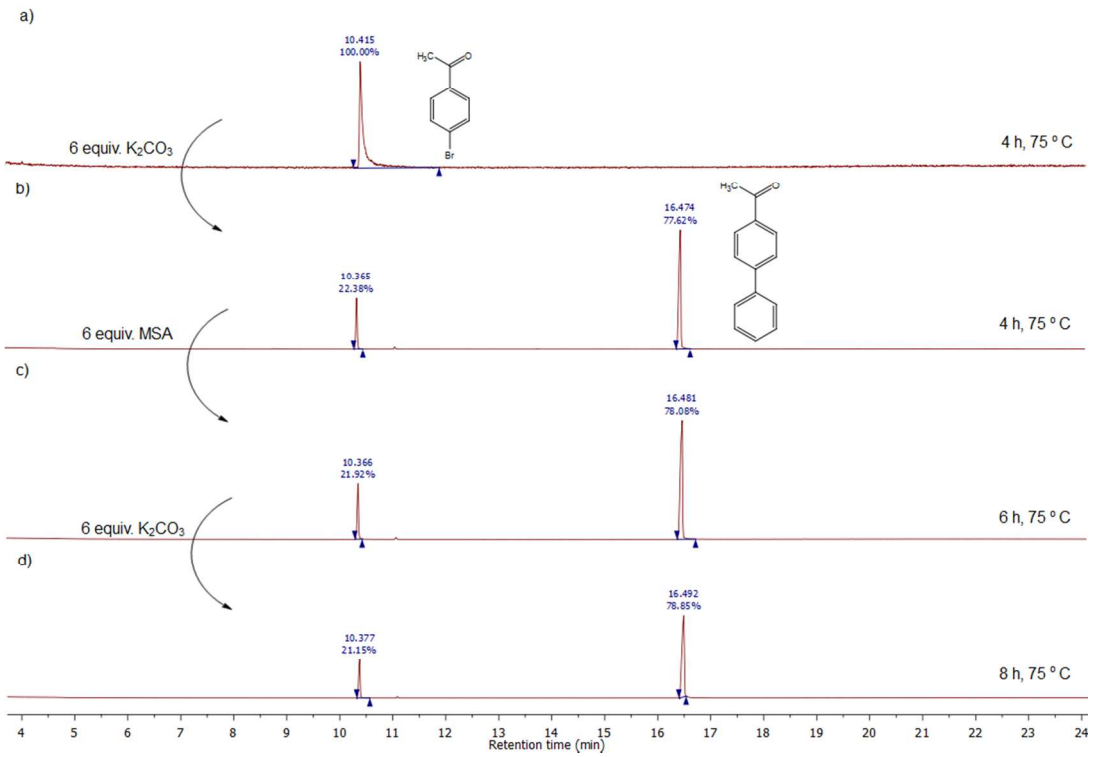

Figure S45. Partial GC traces in $CHCl_3$ showing a) the mixture of catalyst $Pd(OAc)_2$ (2 % mol + 4% mol of ligand), functionalised bromoaryl and phenyl boronic acid after 4h heating at 75 °C without the base; b) the mixture after addition of 6 equiv. of base and 4h heating at 75 °C; c) the neutralized mixture after 6h heating at 75 °C d) the mixture with 6 equiv. of base and 8h of heating at 75 °C.

Acid-base on/off experiment with $Pd(PPh_3)_2Cl_2$, bromo aryl and phenylboronic acid

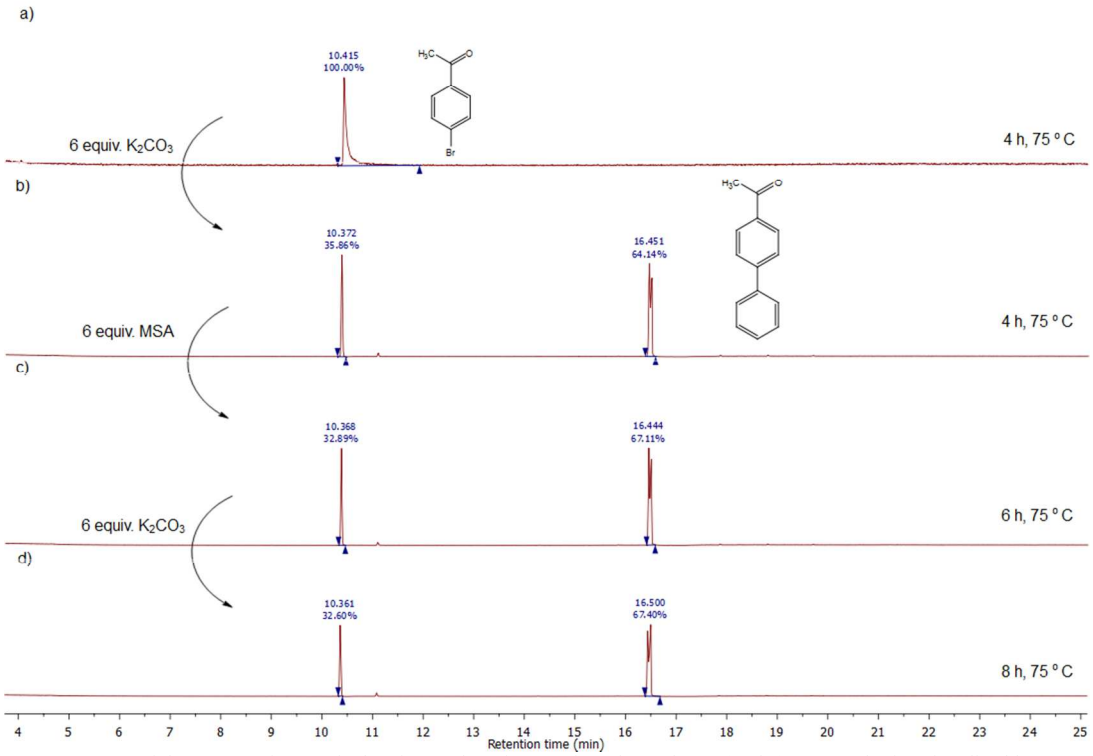

Figure S46. Partial GC traces in $CHCl_3$ showing a) the mixture of catalyst $Pd(PPH_3)_2Cl_2$ (0.2 % mol), functionalised bromoaryl and phenyl boronic acid after 4h heating at 75 °C without the base; b) the mixture after addition of 6 equiv. of base and 4h heating at 75 °C; c) the neutralized mixture after 6h heating at 75 °C d) the mixture with 6 equiv. of base and 8h of heating at 75 °C.

5. Investigation of different reaction conditions employed for the SM reaction:

- Solvent:

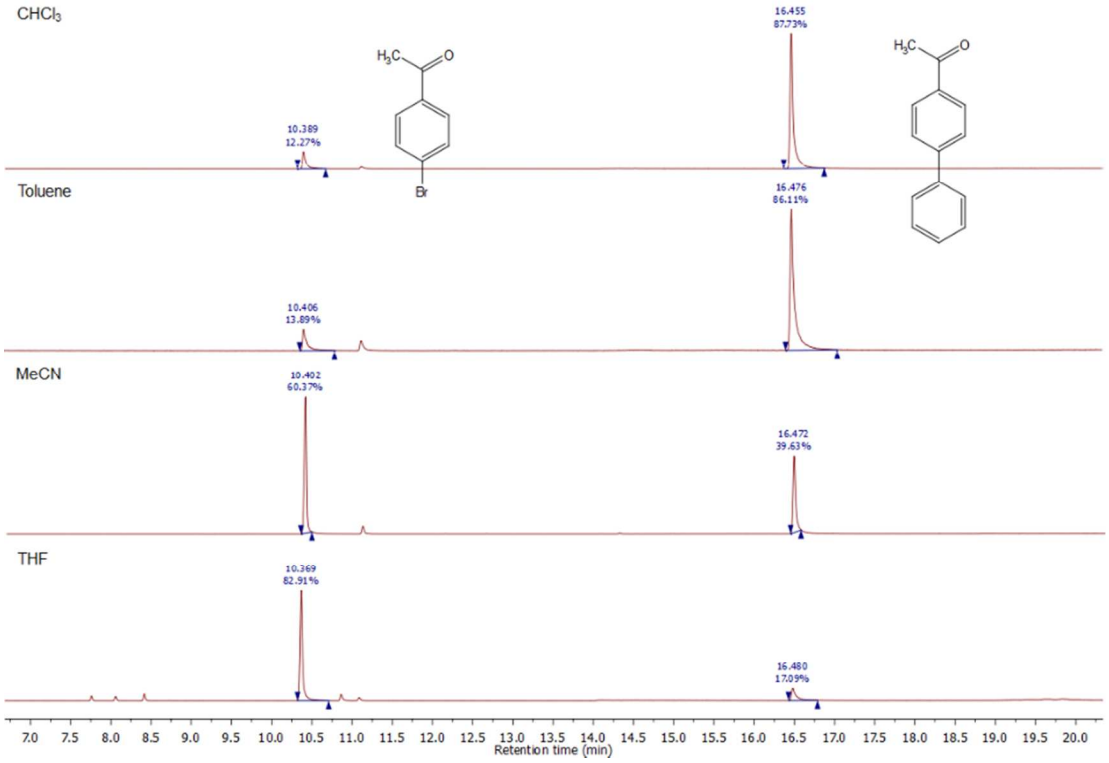

Figure S47. GC chromatograms showing the conversion of 4'-bromoacetophenone in various solvents: $CHCl_3$, toluene, MeCN and THF.

- Temperature

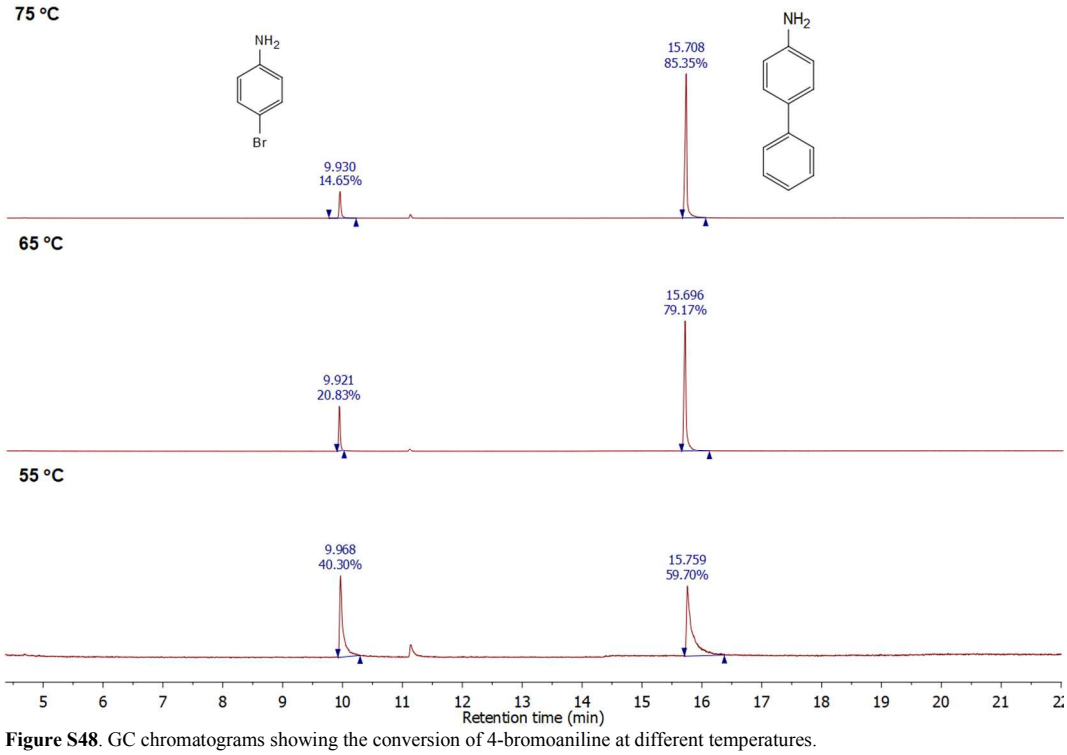

Figure S48. GC chromatograms showing the conversion of 4-bromoaniline at different temperatures.

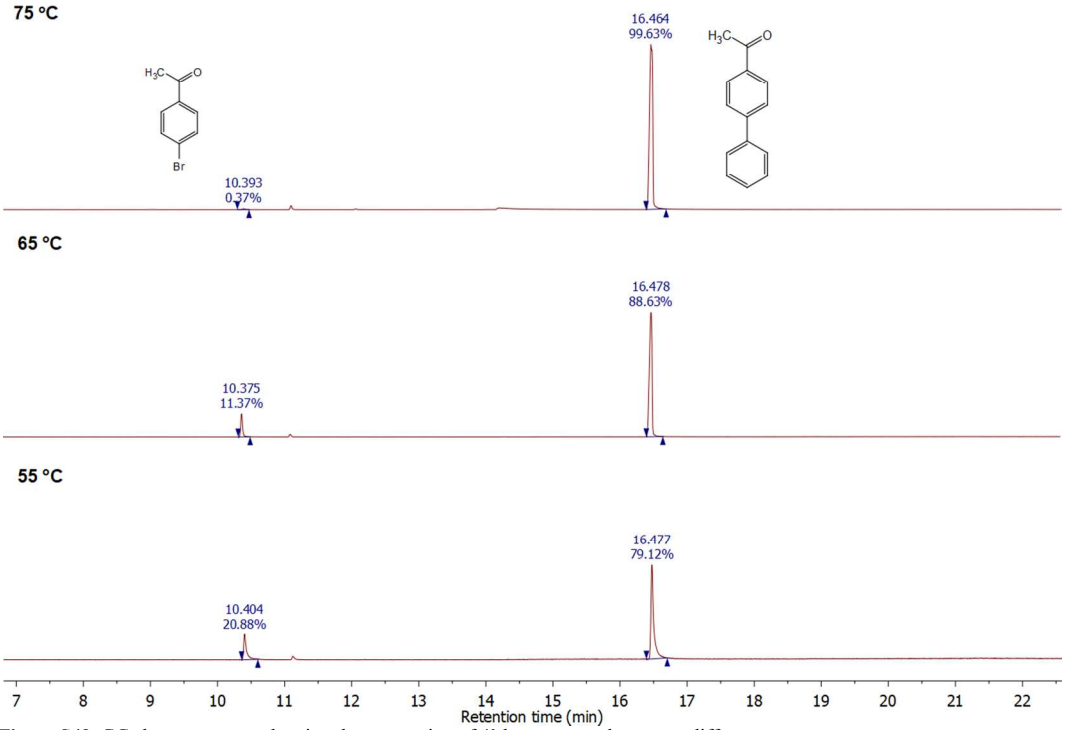

Figure S49. GC chromatograms showing the conversion of 4'-bromoacetophenone at different temperatures.

- catalyst loading – 1 % mol Pd[**L2**]$_2$

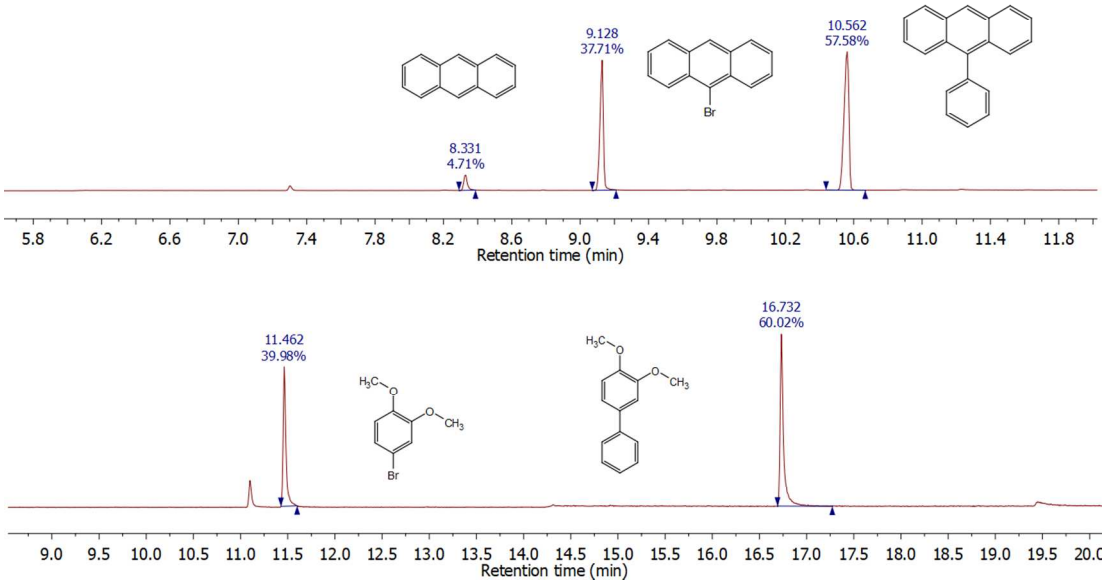

Figure S50. GC chromatograms showing the conversion of 9-bromoanthracene and 4-nitroveratrole for 1 mol % of catalyst Pd[**L2**]$_2$.

6. Spectrophotometry

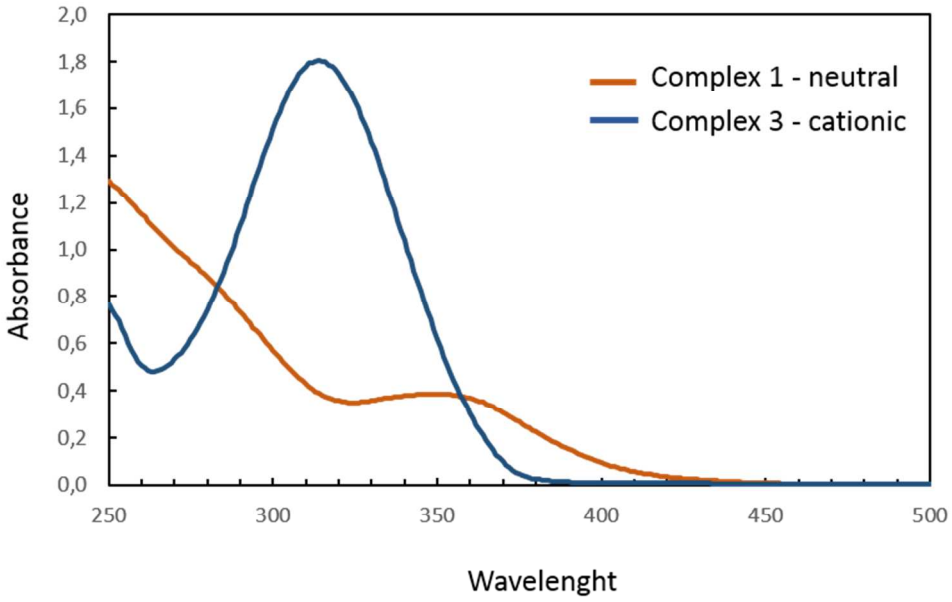

Figure S47. UV-Vis absorption spectra of complex 2 and 4 recorded at 1×10^{-5} M in $CHCl_3$.

7. General experimental procedure for the synthesis and isolation of 4-Aminobiphenyl as a model SM reaction product:

The sealed tube was charged with phenylboronic acid (20.0 mg, 0.164 mmol), 4-Bromoaniline (23.4 mg, 0.136 mmol), K_2CO_3 (45.9 mg, 0.327 mmol) in 0.2 ml H_2O, and **2** (0.01 mol %) as a solution in 4 ml $CHCl_3$. The mixture was stirred at 75 ◦C for 4h. The mixture was added to water (10 mL) and ethyl acetate (10 mL), followed by extraction three times with ethyl acetate (3x10mL). The combined organic fractions were combined, dried over $MgSO_4$ and the solvent was removed under reduced pressure. After removal of the solvent, the resulting residue was purified by flash chromatography on a silica.

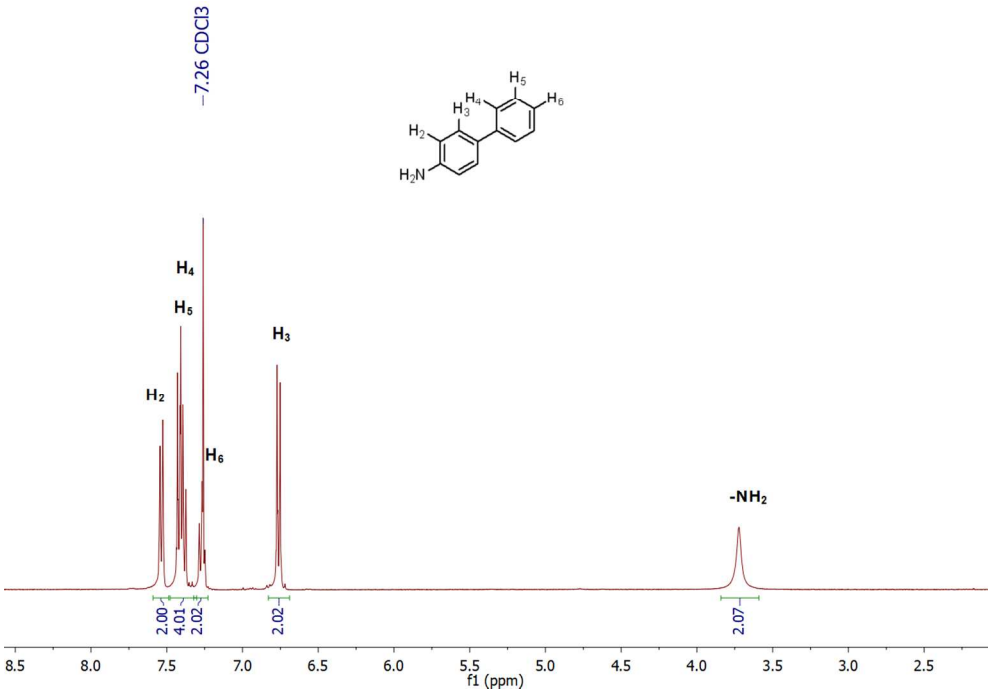

Figure S48. 1H NMR spectrum (400 MHz, CDCl3) of 4-Aminobiphenyl.

4-Aminobiphenyl: Prepared by general procedure and purified by flash chromatography on silica gel using petroleum ether or PE/EtOAc as the eluent to obtain the desired products. Greyish solid; ^{1} H NMR (400 MHz, $CDCl_3$): δ 3.71 (s, 2 H), 6.76 (d, J = 8.5 Hz, 2 H), 7.27(t, J = 7.4 Hz, 1 H), 7.45 – 7.35 (m, 4 H), 7.54 (d, J = 7.0 Hz, 2 H). Yield of the isolated material: 18,54 mg (81 %). Yield observed by GC analysis: 85%.